HEAT TRANSFER AND HEAT EXCHANGERS

1. Introduction

In many branches of engineering and technology, it is of great interest to be able to calculate temperature distributions and heat fluxes. In order to design, size, and rate heat exchangers, eg, condensers, evaporators, and radiators, analysis of the heat transfer is needed. Huge applications of this type of equipment appear frequently in heat and power generation, process industries, automotive engineering, etc. Design and sizing of air conditioning equipment, electronics, cooling, and insulation of buildings require knowledge of heat transfer. There are many heat transfer problems present for vehicles.

To enable stress and strain analysis in equipment exposed to high temperature, analysis of the temperature field and heat loads is needed. In manufacturing, production, and treatment of materials, heat transfer is also important.

Cooling of electronics and other equipment carrying electrical currents is an important application area of heat transfer. In combustion devices, Heat transfer by thermal radiation and convection is also of significance in combustion devices.

Processing and treatment of food require analysis of heat and mass transfer.

2. Heat Transfer Theory

Heat is a form of energy that is always transferred from the hot to the cold part within a substance or from a body at a high temperature to another body at a lower temperature. The bodies do not need to be in contact, but a difference in temperature must exist.

In some cases, the amount of heat transferred can be determined simply by applying basic relations or laws of thermodynamics and fluid mechanics. In other cases, where the mechanisms of the heat transport are not completely known, methods of analogy or empirical methods based on experiments are applied.

Heat can be transferred by three different means, namely, heat conduction, convection, and thermal radiation, see Figure 1.

Heat conduction is a process where the energy transfer from a region at a high to a low temperature region is governed by molecular motion, as in solid bodies and fluids (gases and liquids) at rest, and by movement of electrons as for metals. The heat transfer rate $\dot{Q}$ is for the plane wall in Figure 1 written as

$$\dot{Q} = \lambda A \frac{t_1 - t_2}{b} \tag{1}$$

In equation 1, λ (or k) is the thermal conductivity (W/mK), A is the area through which heat is passing, b is the wall thickness, and t is temperature.

Typical values of the thermal conductivity are given in Table 1 (1,2).

When a fluid is flowing along an exterior surface or inside a duct, and since the temperatures of the fluid and the solid surface are different, the amount of heat being exchanged is affected by the macroscopic fluid motion. This type of

heat transfer is called convection. Depending on how the macroscopic fluid movement is created, forced convection or free (natural) convection prevails. In some cases, both forced and free convection occur simultaneously. The process is then called mixed convection or combined forced and free convection. The heat transfer rate $\dot{Q}$ is written by introduction of the convective heat transfer coefficient h (or α) (W/m^2K) as

$$\frac{\dot{Q}}{A} = \alpha(t_f - t_w) = h(t_f - t_w) \tag{2}$$

In equation 2, t_f is the fluid temperature and t_w is the wall temperature.

Typical values of h or α are given in Table 2 for air and (1–3).

In the forced convection heat transfer, the heat transfer coefficient, α or h, depends on the fluid velocity, type of fluid, and geometry. The flow field may be classified as laminar or turbulent. Laminar flow is generally characterized by low velocities and turbulent flow by high velocities. It is customary to use the Reynolds number, *Re*, to identify whether a flow is laminar or turbulent.

2.1. Dimensionless Numbers in Convection Heat Transfer Analysis. *Reynolds Number.* The Reynolds number, *Re*, is named after Osborne Reynolds, who studied the flow of fluids, and in particular the transition from laminar to turbulent flow. This transition was found to depend on flow velocity, viscosity, density, tube diameter, and tube length. By using a nondimensional group, defined as $\rho VD_i/\mu$, the transition from laminar to turbulent flow for any internal flow takes place at a value of $\sim$2300. Hence, the dimensionless Reynolds number is commonly used to describe whether a flow is laminar or turbulent. Thus for a tube flow one has

$$Re = \rho VD_i/\mu \tag{3}$$

where ρ is the fluid density, V the average flow velocity, D_i the tube inside diameter, and μ is the dynamic viscosity of the fluid.

Noncircular tubes are often used in various compact heat exchangers and the Reynolds number in these tubes is of interest. For noncircular tubes, eg, square, rectangular, elliptic, and triangular tubes, the so-called hydraulic diameter, D_h, defined as

$$D_h = \frac{4A}{P_m} \tag{4}$$

is used in the definition of the Reynolds number where A and P_m are the cross-sectional area and the wetted perimeter of tube, respectively. The noncircular tubes are used in compact heat exchangers mainly because of their geometry, ie, a greater surface area per unit volume of the exchanger is possible.

Nusselt Number. Empirical correlations can be obtained for a particular size of tube diameter and particular flow conditions. To generalize such results and to apply the correlations to different sizes of equipment and different flow conditions, the heat transfer coefficient, h or α, is traditionally

nondimensionalized by the use of the Nusselt number, Nu, named after Wilhelm Nusselt,

$$Nu = \frac{hL}{k_f} = \frac{\alpha L}{k_f} \tag{5}$$

where L is a characteristic length for the flow geometry under consideration, eg, for flow inside a tube; L is equal to the tube internal diameter (D_i); and k_f is the thermal conductivity of the fluid.

Prandtl Number. The Prandtl number, Pr, is the ratio of the kinematic viscosity, ν, to the thermal diffusivity, a.

$$Pr = \frac{\nu}{a} = \frac{\mu c_p}{k_f} \tag{6}$$

Unlike the Reynolds and Nusselt numbers, which depend on flow conditions, the Prandtl number is independent of flow conditions and is a thermophysical property of a fluid. Values of the Prandtl number of air and water at room temperature are $\sim$0.7 and 7.0, respectively. The Prandtl number of air remains almost constant with increasing temperature, whereas that of water decreases significantly, ie, for water $Pr = 1.9$ at 93°C. Some well-known heat transfer fluids have relatively high Prandtl numbers. For example, the Prandtl numbers of glycerin, ethylene glycol, and engine oil are 12.5, 204, and 10,400, respectively (1,2).

2.2. Correlations for Convective Heat Transfer. In the design or sizing of a heat exchanger, the heat transfer coefficients on the inner and outer walls of the tube or duct must be calculated. Summaries of the various correlations for convective heat transfer coefficients for internal and external flows are given in Tables 3 and 4, respectively, in terms of the Nus. In addition, the friction coefficient is given for the determination of the pumping requirement.

The convective heat transfer coefficient for laminar flow in noncircular ducts can be calculated from empirically or analytically determined Nusselt numbers, as given in Table 5. For turbulent flow, the circular duct data with the use of the hydraulic diameter, defined in equation 4, may be used.

Composite Plane Wall and Circular Tube. In many engineering applications, a plane wall is composed of more than one material as shown in Figure 2. On the hot and cold sides, usually convective heat transfer occurs. All thermal resistances are in series, so the total heat transfer rate is given by equation 7.

$$\dot{Q} = \frac{t_{f_1} - t_{f_2}}{\frac{1}{\alpha_1 A} + \frac{b_1}{\lambda_1 A} + \frac{b_2}{\lambda_2 A} + \frac{b_3}{\lambda_3 A} + \frac{1}{\alpha_2 A}} \tag{7}$$

Tubes are frequently appearing in engineering practice, eg, tubular heat exchangers, and for a composite wall, as shown in Figure 3, the corresponding expression for the heat transfer rate reads:

$$\dot{Q} = \frac{t_{f_i} - t_{f_o}}{\frac{1}{2\pi r_1 L \alpha_i} + \frac{1}{2\pi\lambda_1 L}\ln\frac{r_2}{r_1} + \frac{1}{2\pi\lambda_2 L}\ln\frac{r_3}{r_2} + \frac{1}{2\pi r_3 L \alpha_o}} \tag{8}$$

Extended Surfaces or Fins. An extended surface means a solid body that experiences heat transfer by conduction within its boundaries and by convection (and/or radiation) between its boundaries and the surroundings. In most applications, the extended surface is used to enhance the heat transfer rate between a solid and an adjoining fluid. Such an extended surface is termed a fin. Different fin configurations exist, and in Figure 4 annular fins on a tube and rectangular fins on a plane wall are shown.

Concepts of fin effectiveness and efficiency are introduced to calculate the fin performance. The effectiveness is defined as the ratio of the fin heat transfer rate to the heat transfer that would exist without the fin. The fin efficiency φ is defined as the ratio of the fin heat transfer rate to the heat transfer rate of an identical fin, but with infinite thermal conductivity. Thus the value of φ is in the interval $[0, 1]$. For the configurations in Figure 4 the heat transfer rate is given by

$$\dot{Q} = \alpha(t_b - t_f)(A_b + \varphi A_{\text{fins}}) \tag{9}$$

For rectangular fins, the fin efficiency can be calculated according to

$$\varphi = \frac{\tanh mL}{mL} \tag{10}$$

where m is $m = \sqrt{\dfrac{2\alpha}{\lambda b}}$($b$ is the fin thickness, λ the fin thermal conductivity and α the heat transfer coefficient).

For annular fins as in Figure 4 the fin efficiency can conveniently be determined from Figure 5 below.

Thermal Radiation. Heat transfer by radiation does not require any medium to propagate. The heat transfer between two surfaces by radiation is in fact maximum when no media is present between the surfaces. Radiation may occur between surfaces, between a surface and a participating medium like a gas. The heat exchange due to radiation is governed by electromagnetic waves according to Maxwell's theory or in the form of discrete photons according to Planck's hypothesis. For surfaces in an enclosure, the radiative heat exchange for any of the surfaces is given by equations 11 and 12.

$$\dot{Q}_i = A_i \frac{\varepsilon_i}{1 - \varepsilon_i}(E_{\text{B},i} - J_i) \tag{11}$$

$$\dot{Q}_i = A_i \sum_k F_{ik}(J_i - J_k) \tag{12}$$

where $E_{\text{B},i}$is the blackbody radiation of surface i given by the Stefan–Boltzmann law, J_i is the radiosity of surface i, F_{ik} is the view factor between surfaces i and k, A_i is the area of surface i, and ε_i is the emissivity of surface i. In conventional heat exchangers, radiative heat transfer may not be important, but in high temperature applications it may have an effect and sometimes gaseous radiation may be present as well.

3. Heat Exchangers

3.1. Introduction. Heat exchangers are equipment being used for transfer of heat between two or more fluids at different temperatures. Several types of heat exchangers have been developed and are being used in power plants, as refrigerators and automotive heat exchangers, heat pumps, air conditioning, chemical process industries, etc. In so-called shell-and-tube heat exchangers and vehicle radiators, heat is primarily transferred by convection and conduction from a hot fluid to a cold one, which are separated by a metallic wall. In evaporators and condensers, the heat transfer due to evaporation and condensation is the primary mechanism. In some heat exchangers, eg, cooling towers, the hot fluid (water) is cooled by direct mixing with the cold fluid (air). Design and sizing of heat exchangers are complicated engineering work. Convective heat transfer, pressure drop, estimation of the thermal performance and economical issues are important at the final design. For big units in power plants or chemical process industries, the cost (investment and operation) might be an important issue while in applications for space and aircraft, the weight and size (compactness) might be most important. In this article, the functioning and classification of heat exchangers are presented. Methods for analysis, sizing, and rating are provided.

3.2. Classification of Heat Exchangers. Heat exchangers may be classified in various ways. Here the method introduced in (4) is followed. Heat exchangers are distinguished by (a) how the heat transfer process occurs; (b) compactness (heat transfer area per unit volume); (c) design principle; (d) flow process; and (e) mechanism for the heat exchange.

Heat Transfer Process. Heat exchangers may operate in direct contact with the fluids or by indirect contact. If direct contact prevails, the heat transfer occurs between two immiscible fluids, eg, a gas and a liquid that are forced into contact. Cooling towers are such examples.

Cooling towers are often applied to cool waste heat from industrial processes. Commonly, both natural convection and forced convection towers are used. Figure 6 shows a cooling tower in which natural convection prevails. Water is sprayed directly into the air stream that is moving upward by natural convection.

The falling water droplets are cooled by convection, but also by evaporation of the liquid water. In the tower, there are several decks that among other things slow down the droplet downward motion. Therefore the exposure time to the cold air stream is increased. Cooling towers may have heights of >100 m. For cases with forced convection, the air stream is forced through the tower by fans. The fans might be located at the top of the tower and then the air is sucked through the tower. In other designs, the fans are at the bottom of the tower and the air is pressed through the tower. The increased air circulation will increase the cooling capacity.

In heat exchangers having indirect contact, the hot and cold fluids are separated by an impermeable surface. The fluids are not mixed. This is the most common heat exchanger type and sometimes these are referred to as surface heat exchangers.

Compactness. The ratio between the heat transfer area (on one side of the heat exchanger) and the volume is used as a measure of the compactness of the heat exchanger. If this ratio, A/V, is >700 m^2/m^3, the heat exchanger is said to be compact. Radiators in private cars has typically 1100 m^2/m^3 and in some glass–ceramic heat exchangers A/V might be 6500 m^2/m^3. The human lungs have $A/V \sim 20{,}000$ m^2/m^3 and are the most compact heat mass exchanger. Shell-and-tube heat exchangers, which are very common in the process industries, have $A/V \sim 70–500$ m^2/m^3 and are usually not considered as compact.

A reason to apply compact heat exchangers is that a high A/V value diminishes the volume. When heat exchangers are used in cars, trucks and buses, marine vehicles, aircraft and space ships, cryogenic systems, as well as in air conditioning, the weight and size (volume) and thus compactness, is a key issue. In gas–liquid heat exchangers, the heat transfer coefficient on the gas side is much less than that on the liquid side. To enable the transfer of a certain heat power, the surface of the gas side must be increased. Fins or extended surfaces of various geometries are then being used. Figure 7 shows a typical compact heat exchanger.

Sometimes the amount of heat transferred per unit volume (W/m^3) is used as a measure of the compactness.

Types of Design. Heat exchangers may also be classified according to the design. So, for example, one speaks about shell-and-tube heat exchangers, plate heat exchangers, finned plate heat exchangers, finned tubular heat exchangers, and regenerative heat exchangers.

Shell-and-tube heat exchangers are the most common heat exchangers and are manufactured in a wide range of sizes, flow arrangement, etc. The manufacturing method is relatively simple and if common carbon steels can be used, the heat exchanger might be very cheap. The most common layout consists of a large number of tubes placed in a cylindrical shell (thus the name shell-and-tube heat exchanger). Figure 8 shows a principle sketch of a simple shell-and-tube heat exchanger, where one of the media is flowing in the tubes (tube side) and the other one is flowing on the outside of the tubes (shell side fluid). Typical components in such heat exchangers are the tube bundle, the shell, distribution and collection headers, and the baffles.

The baffles are used to support the tubes, guide the flow so the outside surfaces of the tubes are mainly approached in cross-flow, and to increase the turbulence in the flow field. Different types of baffles exist. The design, the distance between and the geometry of the baffles depend on the flow velocity, permitted pressure drop on the shell side, required support for the tubes, and the risk for flow induced vibrations. The heat exchange may occur from one liquid to another from a liquid to a gas or from a gas to another gas. Also, two-phase flows on either side is possible. Liquid–liquid is the most common case, but also liquid–gas occurs frequently. In the latter case, usually fins or extended surfaces are used on the gas side as the convective heat transfer coefficient is low there.

Plate heat exchangers (PHEs) are built up by a number of thin plates assembled together in a package. The plates can be smooth or more commonly corrugated in some way. Plate heat exchangers may normally not operate at as high pressure and temperatures as shell-and-tube heat exchangers. The

reason is because often a gasket is used to seal between adjacent plates. The compactness is ~120–250 m^2/m^3. Figure 9 shows a typical PHE.

Finned plate heat exchangers are shown in Figure 10. The compactness can be as high as 6000 m^2/m^3. Most commonly, this heat exchanger type is for gas-to-gas exchange. Louvered, perforated or so-called offset-strip fins are used to separate the plates and create flow channels. Cross-flow, counterflow, or parallel flow arrangements are common.

Finned tubular heat exchangers are used as a high operating pressure prevails for one of the media or when finned surfaces are needed, eg, for heat exchange between a liquid and a gas. Figure 11 shows two common configurations, one with circular tubes and another with flat tubes. The compactness is usually <350 m^2/m^3.

Regenerative heat exchangers might be static or dynamic. The static type consists of a porous material through which the hot and cold fluids are flowing in alternate fashion. Switch equipment controls the periodic flow of the two fluids. The hot fluid heats up the porous material that in the next sequence heats up the cold fluid. This process is repeated periodically. In the dynamic type, the heat exchanger core is rotating in such a way that part of it is periodically exposed to the hot fluid and then successively to the cold fluid. Rotating regenerative heat exchangers are used as preheaters in heat and power plants and as heat recovery units in air conditioning systems. The heat exchanger is most suitable for gas to gas heat exchange because for gases only the heat capacity of the core is much larger than those of fluids.

Classification Based on Flow Process. This section present the most common flow processes considered for classification of heat exchangers. Cocurrent flow or parallel flow means that the fluids are entering the heat exchanger at the same place and are flowing in the same direction along the exchanger, finally leaving the heat exchanger at the same place. Figure 12 shows a principle sketch of a parallel flow heat exchanger.

Counterflow in heat exchangers means that the hot and cold fluids are entering the exchanger at different places and flow in opposite directions, which is depicted in Figure 13.

In so-called cross-flow heat exchangers, the fluids are flowing perpendicular to each other, see Figure 14.

The flow field for each media is said to be mixed or unmixed. Figure 15 shows a case where both the hot and cold fluids are flowing through individual channels, ie, the fluid streams cannot pass in the transversal direction. Both fluids are unmixed in this case.

In Figure 16, one medium is flowing in the tubes and cannot move in the transversal direction. This medium is unmixed. The other fluid is flowing across the tubes and is free to move in the transversal direction. This medium is therefore regarded as mixed.

Multipass flow fields are common in heat exchangers, in particular for so-called shell-and-tube heat exchangers. Figure 17 shows some typical arrangements.

Figure 17**a** shows a case with one shell pass and two tube passes, while Figure 17**b** shows an arrangement with two shell passes and four tube passes.

Classification According to the Mechanism for Heat Transfer. The mechanism for heat transfer includes a combination of the mechanisms listed has. (a) Single-phase forced or free (natural) convection; (b) boiling or condensation; and (c) radiation or combined radiation and convection.

3.3. The Overall Heat Transfer Coefficient. Figure 18 shows the principle of heat transfer from the hot to the cold fluid.

The amount of heat transferred is written as

$$\dot{Q} = UA \cdot \Delta t_{\mathrm{m}} = \frac{1}{\mathrm{TR}} \cdot \Delta t_{\mathrm{m}} \tag{13}$$

where U is the overall heat transfer coefficient, A is the area the heat is passing, and Δt_{m} is a mean temperature difference between the hot and cold fluids. The equation $\mathrm{TR} = 1/UA$ is the resistance to heat transfer and is called the total thermal resistance. Between the hot and cold fluids, several resistances appear (2). These resistances are in series and are combined to TR according to

$$\mathrm{TR} = \frac{1}{\alpha_i A_i} + \frac{1}{\alpha_{F_i} A_i} + \frac{b_w}{\lambda_w A_{vl}} + \frac{1}{\alpha_{F_o} A_{\mathrm{o}}} + \frac{1}{\alpha_{\mathrm{o}} A_{\mathrm{o}}} \tag{14}$$

where α_i is the heat transfer coefficient on the inside, A_i is the convective heat transfer area on the inside, α_{F_i} is the fouling factor on the inside, b_w is the thickness of the intermediate solid wall, λ_w is the thermal conductivity of the wall material, A_{vl} is the heat conducting area, α_{F_o} is the fouling factor on the outer surface, α_o is the heat transfer coefficient on the outer surface, and A_o is the convective heat transfer area on the outer side. The resistance due to heat conduction in equations 13 and 14 is only valid for a plane wall or if the material thickness is very small. The heat transfer coefficients α_i and α_o are determined with methods presented in, eg, References 1, 2.

In practical applications, the heat transferring surfaces are fouled by the fluids due to various mechanisms. The fluid type itself is also important. This results in thermal resistances as evident in equation 14. Usually, fouling factors $1/\alpha_{F_i}$ and $1/\alpha_{F_o}$, respectively, are introduced to account for this, see, eg, (5–8). Table 6 [data from (5)] provides some values for the fouling factor.

3.4. The Logarithmic Mean Temperature Difference (LMTD) Method for Analysis of Heat Exchangers. In the thermal analysis of heat exchangers, the total heat transfer rate $\dot{Q}\,[W]$ is of primary interest. To get started, the overall heat transfer coefficient U is assumed to be constant in the whole heat exchanger (average value). The heat transfer rate is then written

$$\dot{Q} = UA \cdot \Delta t_{\mathrm{m}} \tag{15}$$

where A is the heat transferring area and Δt_{m} is a proper average of the temperature difference between the hot and cold fluids. Now one has to find an expression for Δt_{m} so that equation 15 is valid. To enable this, counterflow and parallel flow will be considered.

Counterflow Heat Exchangers. In principle, Figure 19 shows the temperature distributions of the hot and cold fluids in a single pass counterflow heat exchanger.

For the element dA, one has

$$d\dot{Q} = UdA \cdot \Delta t = -(\dot{m}c_p)_h dt_h = -(\dot{m}c_p)_c dt_c \tag{16}$$

where index h means hot fluid and index c means cold fluid.

For the heat capacity, flow rates $\dot{m}c_p$ is the following notations are introduced

$$C_h = (\dot{m}c_p)_h,\ C_c = (\dot{m}c_p)_c \tag{17}$$

The total heat transfer rate $\dot{Q}$ can be written

$$\dot{Q} = C_h(t_{h_{\text{in}}} - t_{h_{\text{out}}}) \tag{18}$$

$$\dot{Q} = C_c(t_{c_{\text{out}}} - t_{c_{\text{in}}}) \tag{19}$$

Δt in equation 16 can be written

$$\Delta t = t_h - t_c \tag{20}$$

The change in Δt is, $d(\Delta t) = dt_h - dt_c$. With equations 15 and 16 one has

$$d(\Delta t) = d\dot{Q} \cdot (\frac{1}{C_c} - \frac{1}{C_h}) \tag{21}$$

By using the first part of equation 16, one has

$$d(\Delta t) = U\,dA\,\Delta t(\frac{1}{C_c} - \frac{1}{C_h})$$

$$\frac{d(\Delta t)}{\Delta t} = U\,dA(\frac{1}{C_c} - \frac{1}{C_h})$$

Integration over the whole heat exchanger gives

$$\int_{\Delta t_{\text{a}}}^{\Delta t_{\text{b}}} \frac{d(\Delta t)}{\Delta t} = \int_0^A U\,dA(\frac{1}{C_c} - \frac{1}{C_h})$$

$$\ln\frac{\Delta t_b}{\Delta t_a} = UA(\frac{1}{C_c} - \frac{1}{C_h})$$

With equations 15, 18 and 19, one obtains

$$\ln\frac{\Delta t_b}{\Delta t_a} = \frac{\dot{Q}}{\Delta t_{\text{m}}}\left(\frac{(t_{c_{\text{out}}} - t_{c_{\text{in}}})}{\dot{Q}} - \frac{(t_{h_{\text{in}}} - t_{h_{\text{out}}})}{\dot{Q}}\right)$$

For Δt_{m}, one finds

$$\Delta t_m = LMTD = \frac{\Delta t_b - \Delta t_a}{\ln \frac{\Delta t_b}{\Delta t_a}}$$

or

$$\Delta t_{\mathrm{m}} = \mathrm{LMTD} = \frac{(t_{h_{\mathrm{out}}} - t_{c_{\mathrm{in}}}) - (t_{h_{\mathrm{in}}} - t_{c_{\mathrm{out}}})}{\ln \frac{(t_{h_{\mathrm{out}}} - t_{c_{\mathrm{in}}})}{(t_{h_{\mathrm{in}}} - t_{c_{\mathrm{out}}})}} \tag{22}$$

Equation 28 gives Δt_{m} for a counterflow heat exchanger. This temperature difference, which also will be applied for other heat exchangers, is called LMTD. Please observe that if the heat capacity flow rates of the fluids are equal, the temperature difference will be constant across the heat exchanger, ie, $> \Delta t = \Delta t_{\mathrm{m}} = (t_{h_{\mathrm{out}}} - t_{c_{\mathrm{in}}}) = (t_{h_{\mathrm{in}}} - t_{c_{\mathrm{out}}})$.

Parallel Flow Heat Exchangers. Figure 20 shows the principal temperature distributions in a single pass parallel flow heat exchanger.

With the notations in Figure 20, it is possible to derive, in a similar manner, an expression for Δt_{m} of a parallel flow heat exchanger.

$$\Delta t_{\mathrm{m}} = \frac{\Delta t_b - \Delta t_a}{\ln \frac{\Delta t_b}{\Delta t_a}}$$

or

$$\Delta t_{\mathrm{m}} = \frac{(t_{h_{\mathrm{in}}} - t_{c_{\mathrm{in}}}) - (t_{h_{\mathrm{out}}} - t_{c_{\mathrm{out}}})}{\ln \frac{(t_{h_{\mathrm{in}}} - t_{c_{\mathrm{in}}})}{(t_{h_{\mathrm{out}}} - t_{c_{\mathrm{out}}})}} \tag{23}$$

Correction Factors for LMTD for Noncounter Flow Heat Exchangers. Commonly, the temperature difference LMTD, according to equation 22 is used independent of the heat exchanger type and the flow arrangement in engineering analysis and design. The heat transfer rate is written as

$$\dot{Q} = UA \cdot F \cdot \mathrm{LMTD} \tag{24}$$

where $F(0 < F \leq 1)$ is a correction factor that accounts for the deviation from the corresponding counterflow arrangement.

Commonly, two parameters P and R are introduced. These represent an efficiency or goodness number and the ratio between the heat capacity flow rates, respectively.

One has

$$P = \frac{t_{c_{\mathrm{out}}} - t_{c_{\mathrm{in}}}}{t_{h_{\mathrm{in}}} - t_{c_{\mathrm{in}}}} \tag{25}$$

and

$$R = \frac{(\dot{m}c_p)_c}{(\dot{m}c_p)_h} \tag{26}$$

With equations 18 and 19 the ratio R can be written as

$$R = \frac{t_{h_{\text{in}}} - t_{h_{\text{out}}}}{t_{c_{\text{out}}} - t_{c_{\text{in}}}} \tag{27}$$

The correction factor F depends on P and R, as well as on the heat exchanger type. Analytical expressions are available in the international literature for a number of cases. The mathematics and the algebra to derive the expressions is quite extensive. Here, only some results are presented in a few figures, and from these F can be determined.

Figure 21 gives F for a shell-and-tube heat exchanger with one shell pass and multiples of two tube passes (2, 4, 6, 8, ..., $2n$ tube passes). In Figure 22, F is provided as a function of P and R for a shell-and-tube heat exchanger with two shell passes and four tube passes (or multiples of four tube passes), while Figure 23 presents F for a cross-flow heat exchanger where both fluids are unmixed. Figure 24 gives F for a cross-flow heat exchanger where one fluid is unmixed while the other is mixed.

For technical applications it is improper to use a heat exchanger with $F \leq 0.75$. If $F > 0.75$ can not be achieved for a certain design, one should select another heat exchanger type. For $F < 0.75$ it is clear from the graphs that the curves become almost vertical, which means that small variations in the temperatures or flow rates will result in great differences in the performance of the heat exchanger. More detailed information concerning the correction factor F can be found in References 9–12.

3.5. The ε-NTU Method for Analysis of Heat Exchangers. In the analysis of the performance of a certain heat exchanger, the amount of heat being transferred, outlet temperatures of the fluids, and the pressure drops are of most interest. At the design and sizing stage of a heat exchanger, the heat transferring area and other dimensions are determined in such a way that a prescribed heat flow can be transferred and the pressure drops are within permitted limits.

If the inlet and outlet temperatures of the hot and cold fuids are given, the LMTD method is quite suitable. In other cases, the so-called ε-NTU method is more appropriate. This method was originally developed by Kays and London 1955 (13).

The efficiency or effectiveness ε is defined as

$$\varepsilon = \frac{\text{real heat transfer rate}}{\text{maximum possible heat transfer rate}} = \frac{\dot{Q}}{\dot{Q}_{\max}} \tag{28}$$

The theoretical maximum heat transfer rate states that the fluid with the lowest heat capacity flow rate receives–gives up if its outlet temperature becomes equal

to the inlet temperature of the other fluid. This means $\dot{Q}_{\max} = C_{\min}(t_{h_{\text{in}}} - t_{c_{\text{in}}})$. With the notations already introduced, one has

$$\varepsilon = \frac{C_h(t_{h_{\text{in}}} - t_{h_{\text{out}}})}{C_{\min}(t_{h_{\text{in}}} - t_{c_{\text{in}}})} = \frac{C_c(t_{c_{\text{out}}} - t_{c_{\text{in}}})}{C_{\min}(t_{h_{\text{in}}} - t_{c_{\text{in}}})} \tag{29}$$

where $C_{\min}$ is the smallest value of C_h och C_c.

From equations 28 and 29 it follows that

$$\dot{Q} = \varepsilon\, C_{\min}(t_{h_{\text{in}}} - t_{c_{\text{in}}}) \tag{30}$$

The number of transfer units (NTU) is defined as

$$\text{NTU} = \frac{UA}{C_{\min}} \tag{31}$$

This dimensionless number (originally introduced by W. Nusselt) expresses the ratio between the heat capacity of the heat exchanger [W/K] and the smallest heat capacity flow rate $C_{\min} = (\dot{m}c_p)_{\min}$.

Now, consider a counterflow heat exchanger. Equations 31, 15 and 22 give

$$\text{NTU} = \frac{\dot{Q}/\text{LMTD}}{C_{\min}} \tag{32}$$

The temperature differences in LMTD, see equation 22, can be rewritten as

$$(t_{h_{\text{out}}} - t_{c_{\text{in}}}) - (t_{h_{\text{in}}} - t_{c_{\text{out}}}) = (t_{h_{\text{out}}} - t_{h_{\text{in}}}) - (t_{c_{\text{in}}} - t_{c_{\text{out}}}) = -\frac{\dot{Q}}{C_h} + \frac{\dot{Q}}{C_c} = \dot{Q}(\frac{1}{C_c} - \frac{1}{C_h}) \tag{33}$$

$$\frac{(t_{h_{\text{out}}} - t_{c_{\text{in}}})}{(t_{h_{\text{in}}} - t_{c_{\text{out}}})} = \frac{-(t_{h_{\text{in}}} - t_{h_{\text{out}}}) + (t_{h_{\text{in}}} - t_{c_{\text{in}}})}{(t_{h_{\text{in}}} - t_{c_{\text{out}}}) + (t_{c_{\text{in}}} - t_{c_{\text{out}}})} = \frac{-\dot{Q}/C_h + \dot{Q}/(\varepsilon C_{\min})}{\dot{Q}/(\varepsilon C_{\min}) - \dot{Q}/C_c} = \frac{C_c(C_h - \varepsilon C_{\min})}{C_h(C_c - \varepsilon C_{\min})} \tag{34}$$

With equation 22, 32, 33 and 34, one obtains

$$\text{NTU} = \frac{1}{C_{\min}} \frac{\ln(\frac{C_c}{C_h}\frac{C_h - \varepsilon C_{\min}}{C_c - \varepsilon C_{\min}})}{\frac{1}{C_c} - \frac{1}{C_h}} \tag{35}$$

First, assume that $C_{\min} = C_c$, which means $C_{\max} = C_h$. After some algebraic manipulations one achieves

$$\varepsilon = \frac{1 - \exp[-(1 - C_{\min}/C_{\max})\text{NTU}]}{1 - C_{\min}/C_{\max}\exp[-(1 - C_{\min}/C_{\max})\text{NTU}]} \tag{36}$$

If $C_{\min}$ is set to C_h, one will obtain exactly the same result.

Similar calculations can be carried out for other heat exchanger configurations and results are presented in the international literature.

Formulas $\varepsilon = \text{funktion}\,(\text{NTU}, C_{\min}/C_{\max})$ and $\text{NTU} = \text{funktion}\,(\varepsilon, C_{\min}/C_{\max})$, respectively, are provided for several cases in Tables 7 and 8. Note that some of the formulas are exact, while others are approximate. Figures 25 and 26 present some solutions as diagrams. These are suitable for simple engineering calculations and estimations.

Please note that in Figures 25 and 26 and in the Tables 7 and 8, C is the heat capacity flow rate ratio, ie, $C = C_{\min}/C_{\max}$.

3.6. Condensers and Evaporators (Boilers). For cases with condensers and evaporators, the fluid being condensed or evaporated has a constant temperature (saturation temperature). If the effectiveness ε should be finite, the heat capacity flow rate C (C_h eller C_c) must be infinite, because the temperature difference is zero. The parameter $C_{\max}$ is thus infinite and the ratio $C_{\min}/C_{\max} = 0$.

3.7. Compact Heat Exchangers. *Heat Transfer and Friction Factor.* In the section on classification of heat exchangers, it was said that a heat exchanger is compact when the ratio between the heat transferring area and the volume (A/V) was >700 m^2/m^3. Commonly, at least one of the fluids in such heat exchangers is a gas. Many different configurations exist and heat transfer and pressure drop data are available in, eg, Reference 13. In this section, some configurations will be presented and the associated heat transfer and pressure drop data are given. Figure 27 shows the heat transfer coefficient and friction factor on the gas side for a so-called tubular heat exchanger with plane lamellas (also called plate fin-and-tube heat exchangers), while Figure 28 shows corresponding data for a heat exchanger with circular or annular fins. Please observe that the given data are only valid for specified dimensions that are given in each Figures. In these Figures, the Stanton number St and the Reynolds number are defined as

$$St = \frac{\alpha}{Gc_p} \quad Re = \frac{GD_h}{\mu} \tag{37}$$

where G is the mass velocity which is given by

$$G = \frac{\dot{m}}{A_{\min}} \tag{38}$$

where $\dot{m}$ is the mass flow rate and $A_{\min}$ is the minimum cross-flow area. The hydraulic diameter is defined as

$$D_h = 4\frac{A_{\min}L}{A} \tag{39}$$

where A is the total heat transferring area and L is the depth of the heat exchanger in the main flow direction.

Tubular heat exchangers in staggered arrangement and with plane fins, as shown in Figure 27, are common in, eg, air conditioning units and refrigeration equipment. Several correlations for heat transfer and friction factor are available in the literature (14). Gray and Webb (15) suggest the following correlation:

$$St = 0.14\,Re_D^{-0.328}(S_t/S_l)^{-0.502}(s/D)^{0.0312}\,Pr^{-2/3} \tag{40}$$

This equation is valid for four or more tube rows in the main flow direction. For fewer tube rows, N, a correction is recommended as

$$St_N/St = 0.991(2.24\,Re_D^{-0.092}(N/4)^{-0.031})^{0.607(4-N)} \tag{41}$$

The Reynolds number is calculated as

$$Re_D = \frac{GD}{\mu} \tag{42}$$

where D is the outer diameter of the tubes. Other notations are given in Figure 29.

The friction factor is splitted up in two parts, which can be related to the pressure drop over the fins, f_f, and the pressure drop over the tubes, f_t, respectively. The friction factor, f_f, is calculated as

$$f_f = 0.508\,Re_D^{-0.521}(S_t/D)^{1.318} \tag{43}$$

and f_t can be calculated according to the correlation for tube bundles by Zukauskas and Ulinskas (16). A somewhat simpler correlation has been presented by Jakob (15). This relation reads

$$f_t = \frac{4}{\pi}\left(0.25\,\frac{0.118}{(S_t/D-1)^{1.08}}Re_D^{-0.16}\right)(S_t/D-1) \tag{44}$$

The total friction factor is calculated according to

$$f = f_f\frac{A_f}{A_o} + f_t\left(1-\frac{A_f}{A_o}\right)\left(1-\frac{\delta}{p_f}\right) \tag{45}$$

where A_f is the fin area and A_o the total area on the gas side, ie, the fin area plus the tube area.

The correlation by Gray and Webb is valid for $400 \le Re \le 24,700$, $1.97 \le S_t/D \le 2.55$, $1.70 \le S_l/D \le 2.58$ och $0.08 \le s/D \le 0.64$.

Correlations for friction and heat transfer on the gas side in tubular heat exchangers with plane fins, Figure 28, are available in Reference 16. Data for other fin geometries are available in Reference 17.

By using the heat transfer data (α from St) for the gas side, eg, from Figure 27, Figure 28 and equation 40, and the heat transfer coefficient for inside tube flow (2) the thermal resistance ($1/UA$) for the heat exchanger can be calculated. The LMTD-method or the ε-NTU method can then be applied for design and sizing or analysis of the heat exchanger.

As the thermal resistance on the gas side is determined, the fin efficiency has to be considered, (2). The total resistance (except fouling factors) is written as

$$\frac{1}{UA} = \frac{1}{\varphi_o A_o \alpha_o} + \frac{b_w}{\lambda_w A_{vl}} + \frac{1}{\alpha_i A_i} \tag{46}$$

(In equation 46 it is assumed that only the gas side (outer surface) has fins while the inside is smooth) The overall efficiency on the gas side is related to the fin efficiency according to

$$\varphi_o = 1 - \frac{A_f}{A_o}(1 - \varphi) \tag{47}$$

A_o is the total heat transferring area on the gas side.

Pressure Drop in Compact Heat Exchangers. The pressure drop on the gas side in compact heat exchangers, like those in Figures 27 and 28, is usually splitted up in three components, namely, the frictional loss, acceleration of the fluid, and inlet and outlet losses. For tubular heat exchangers with plane fins as in Figure 28 and if the gas is passing the tubes in cross-flow, the pressure drop is calculated as

$$\Delta p = \frac{G^2}{2\rho_{in}} \left[(1 + \sigma^2)(\rho_{in}/\rho_{out} - 1) + f \frac{A}{A_{min}} \frac{\rho_{in}}{\rho_m} \right] \tag{48}$$

In equation 48 ρ_{in} is the density at the inlet, ρ_{out} is the density at the outlet, and G is determined by equation 45. The area ratio σ is determined according to

$$\sigma = \frac{A_{min}}{A_{front}} \tag{49}$$

The average density ρ_m is calculated according to

$$\frac{1}{\rho_m} = \frac{1}{2}\left(\frac{1}{\rho_{in}} + \frac{1}{\rho_{out}} \right) \tag{50}$$

In equation 47, the inlet and outlet losses are included in the friction factor f. For finned plate heat exchangers, see Figure 9, the pressure drop is calculated according to

$$\Delta p = \frac{G^2}{2\rho_{\text{in}}}\left[\begin{matrix}(K_c + 1 - \sigma^2)+ & 2(\rho_{\text{in}} - \rho_{\text{out}} - 1)+ & f\dfrac{A}{A_{\min}}\dfrac{\rho_{\text{in}}}{\rho_{\text{m}}}- & (1 - K_e - \sigma^2)\dfrac{\rho_{\text{in}}}{\rho_{out}} \\ \text{inlet} & \text{acceleration} & \text{friction} & \text{exit}\end{matrix}\right] \tag{51}$$

In equation 58, K_c is a contraction coefficient at the inlet and K_e is an expansion coefficient at outlet. Typical values of K_c and K_e are given in Reference 13.

Trends in Development and Ongoing Research. In Reference 13, heat transfer and pressure drop data are available for a number of configurations for compact heat exchangers. However, end users of heat exchangers require increased compactness and cheaper manufacturing techniques. The heat transferring surfaces then need to be modified or further developed and innovative new surfaces are also of interest. This also requires that new heat transfer and pressure drop data be established. In References 18–22, ongoing R & D works are exemplified.

3.8. Shell-and-Tube Heat Exchangers. So-called shell-and-tube heat exchangers are the most common exchangers in the process industries. The heat power is commonly >1 MW and the heat transferring area might be up to 5000 m^2. Figure 30**a**–**d** show principal sketches of some design layouts.

The advantages commonly associated with shell-and-tube heat exchangers are

- Great flexibility in operating conditions; phase change, condensation, evaporation.
- Robust equipment.
- Huge operating pressure range.
- Thermal stresses can be handled by proper selection of material.
- Fins can be used on the tube surfaces and then the heat transferring area is increased.

Some disadvantages associated with shell-and-tube heat exchangers are

- Risk for flow-induced vibrations.
- Hard to perform an accurate design because the correlations on the shell side suffice of inaccuracies.

The tube length might be 1–20 m and the shell diameter is typically in the range of 0.25–3.1 m. The outer-tube diameter is within 6–51 mm.

3.9. Practical Design Aspects.

Temperature differences: $t_{h_{\text{in}}} - t_{c_{\text{out}}} > 20^\circ\text{C}$, $t_{h_{\text{in}}} - t_{c_{\text{in}}} > 5^\circ\text{C}$

Temperature level: If one of the fluids is at a high temperature, this fluid should be on the tube side, as the number of components to be manufactured as high temperature material will be limited.

Pressure drop: The order of magnitude of Δp is typically 10–500 kPa on both the tube and shell sides, but usually a little less on the shell side.

Pressure level: The fluid with the highest pressure should be on the tube side.

Viscosity: The most viscous fluid should be on the shell side.

Rate of mass flow: The fluid with the smallest rate of mass flow should be on the shell side.

Corrosion: The fluid being most corrosive should be on the tube side to minimize the damage effect.

Fouling: The fluid suspected to foul the surface should be on the tube side.

Heat Transfer and Pressure Drop on the Tube Side. The pressure drop on the tube side consists of expansion and contraction losses at inlets and outlets, losses in U-bends or mixing chambers, and the friction losses in the straight tubes. For long tubes, the friction loss dominates. Standard methods can be used for this calculation, (2). For the other losses, reference is given to handbooks (12). The heat transfer coefficient inside the tubes can also be determined by standard methods as presented in Reference 2 if the tube surfaces are smooth.

Heat Transfer and Pressure Drop on the Shell Side. The flow field on the shell side is quite complicated. This is in principle conjectured in Figures 8, 17, and 30. The fluid is entering the shell side through an inlet pipe and passes across a tube bundle (sometimes an impingement plate is placed just below the inlet pipe to retard the fluid and protect the tubes). The baffles direct the flows, but also support the tubes. Surface gaps are present between the baffles and the inner-shell, as well as between the baffle holes an additional tubes gaps exist. Leakage occurs through these gaps or openings. This means that part of the mass flow is not passing the tubes in cross-flow.

Figure 31 shows Tinker's principle sketch of the flow field, (23). The nonuniformity in flow velocity and direction, as well as the leakage flows, makes a precise calculation of the heat transfer coefficient and the pressure drop difficult. The notations A–F in Figure 31 represent:

A: Leakage flow due to the gaps between baffle holes and tubes.

B: Main flow path, approximately cross-flow.

C: Bypass-flow between tube bundle and inner-shell surface.

E: Leakage flow between baffles and inner-shell surface.

F: (Not marked in Fig. 31): Bypass-flow in streaks as a result of missing tubes in some regions.

Figure 32 shows two examples of baffles.

The baffle distance in the axial direction is typically 0.25 $\times$ shell diameter.

The heat transfer coefficient is calculated according to

$$\alpha_s = c\alpha_{\text{tube bundle}} \tag{52}$$

where $\alpha_{\text{tube bundle}}$ is the heat transfer coefficient for a tube bundle in cross-flow. Such coefficients can be determined as described in References 2, 24, 25. The correction factor c involves several factors considering effects of leakage, bypass flow etc, (12). The order of magnitude for c is $c \sim 0.6$.

The pressure drop on the shell side is spitted up in the pressure drop contributions at the inlet and outlet, cross-flow over the tube bundle, flow in the so-called window sections. A window section is the region between the inner-shell surface and the location where a baffle ends, see also Figure 30. For the tube bundle cross-flow, the pressure drop is calculated as

$$\Delta p_c = \Delta p_{\text{tube bundle}}(N_b - 1)R_1 \tag{53}$$

where $\Delta p_{\text{tube bundle}}$ is the pressure drop across the tube bundle (2,16,24,25), N_b is the number of baffles, and R_1 is a correction factor taking leakage and bypass flow into account (12).

For the inlet and outlet, the pressure drop is written according to

$$\Delta p_e = \Delta p_{\text{tbue bundle}} \frac{N_c + N_{\text{cw}}}{N_c} R_2 \tag{54}$$

where N_c is the number of tube rows in cross-flow between two adjacent baffles, N_{cw} is the number of tube rows in the window section, and R_2 is a correction factor for the bypass flow and the specific conditions at the inlet and outlet regions. For more details, see Reference 12.

In the window section, the pressure drop is calculated from

$$\Delta p_w = \Delta p_{tkw} N_b R_3 \tag{55}$$

where Δp_{tkw} is the pressure drop over the tube bundle in the window section and R_3 is a correction factor for leakage.

The total pressure drop Δp_{tot} is calculated as

$$\Delta p_{\text{tot}} = \Delta p_c + \Delta p_e + \Delta p_w \tag{56}$$

Error Estimations. In the design process of shell-and-tube heat exchangers, it is important to know the accuracy in the calculations of the heat transfer coefficient α_s and the pressure drop Δp_{tot} on the shell side. The parameter α_s is estimated to be accurate within 25%, while Δp_{tot} is accurate only within 40–75%.

Need for Research. As is evident from the presentation above, the uncertainty in the estimations of the heat transfer coefficient and the pressure drop is rather high particularly for the shell side. To improve the correlations and methods to calculate the correction factors is indeed a difficult task because of the complex geometry and complex flow field. The risk of flow induced vibrations at high velocities has to be considered as high velocities are also good for the thermal performance of the heat exchanger. Studies of flow induced vibrations for idealized situations are presented in References 26, 27.

3.10. Plate Heat Exchangers. Plate heat exchangers (plate-and-frame heat exchangers), see Figure 33, is the second most common heat exchanger. These heat exchangers generally have higher heat transfer coefficients (U-value) and higher compactness than shell-and-tube heat exchangers. In

addition, they are more easy to clean, as the whole package can be disassembled. However, the operating pressures and temperatures are lower.

The heat transferring surface consists of a number of plates, see Figures 33 and 34, which are assembled together in a package. Every plate is equipped with a gasket that is fixed in grooves on one side along the plate border. The gasket seals off against the adjacent plate. As is evident in Figure 34, a plate has holes at the corners. With the layout of the gasket and its placement, the flow is controlled so that a stream either enters or passes the channel between two adjacent plates. As the plates are assembled to a package, see Figure 33, the holes and the gaskets create a channel system. The hot and cold fluids are passing and entering every second channel. The operation is most commonly in counterflow. The distance between the plates is very small, typically a few millimeters. A big heat transfer area per unit volume is achieved.

Commonly, the plate surfaces are corrugated, which creates turbulence and enhanced mixing, and as a result the heat transfer coefficient is high. The corrugation also improves the stiffness of the plates, which means that plate material thickness can be made small (typically 0.5–0.6 mm). The thermal resistance in the plates will then be small. The surface pattern is commonly according to two main patterns, namely, the so-called herringbone pattern and the washboard pattern. These are shown in Figure 34. Other patterns exist and combined patterns also are available.

The fundament of a PHE consists of one fixed and one adjustable end plate. The thick end plates are bolted together with the plate package in between. The number of bolts depends on the operating pressure.

The plates can be coupled together in several ways. The plate package can be divided into a number of streaks for the fluids. In Figure 35, a few examples of couplings are shown. Nowadays, PHEs are also manufactured with plates without gaskets. The PHEs are then brazed or welded. For brazed PHEs, vacuum brazing is applied and the contact points are then brazed together creating a strong bond. The operating pressures and temperatures can then be much higher. The disadvantage is that the brazed PHE cannot be disassembled. Figure 36 shows pictures of some brazed PHEs.

Sometimes a thermal length θ is introduced as heat exchangers are discussed. It is defined as

$$\theta = \frac{\Delta t}{\mathrm{LMTD}} \tag{57}$$

where Δt is the temperature difference of one of the fluids and LMTD is the logarithmic mean temperature difference for an ideal counterflow heat exchanger. If Δt is equal to the temperature difference for the fluid with the smallest heat capacity flow rate, θ will be equal to NTU, ie, the number of transfer units.

For plates with a tight pattern, the pressure drop is high and the heat transfer is very efficient. One then has a thermally long channel (high θ). If plates have a more open pattern, the pressure drop will be low and the heat transfer will be worse. Now one has a thermally short channel (low θ). It is possible two assemble plates with different patterns together. The result will be

something in between a long and a short channel in terms of pressure drop and heat transfer performance.

3.11. Regenerative Heat Exchangers. A regenerative heat exchanger has a setup of channels inside a relatively large matrix of a solid material. The hot and cold fluids pass the matrix in an alternating manner. As the hot fluid passes the flow channels in the matrix, heat is transferred to the matrix and the temperature (internal energy) of the matrix is increased. In the next step, as the cold fluid is passing through the matrix heat is transferred to the cold fluid and the matrix is cooled down.

Regenerative heat exchangers are classified as static or dynamic. The dynamic ones have moving parts. In most cases, the matrix is in the form of a planar dish or a drum, see Figure 37. The matrix material is exposed sequentially to the hot and cold fluids. Most commonly, the matrix is rotating. This type is frequently occurring as preheater in heat and power plants (Ljungstrom preheater or regenerator) and for heat recovery in air conditioning units. In a variant of this heat exchanger, the matrix is fixed and instead the inlet and outlet nozzles of the fluids are moving over the matrix cross-section.

Static regenerative heat exchangers have no moving parts except for supply and delivery of auxiliary equipment. Most applications have continuous flows of the hot and cold fluids, and then two matrices are required as well as periodic switching, see Figure 38. At every instant of time, one matrix is in contact with the hot fluid while the other one is exchanging heat with the cold fluid.

Rotating Heat Exchanger for Heat Recovery and Air Preheating. Figure 39 shows the matrix (rotor or wheel) of a typical rotating regenerative heat exchanger. The rotating wheel is built up by two foil systems arranged in a way so that small channels are created. The wheel rotates relatively slow, up to 10 rpm. Usually, $\sim$50% of the front surface is exposed for one of the fluids while the other half is open for the other fluid. Commonly, counterflow operation prevails. The wheel will in a periodic manner be heated up and cooled. In continuous operation, the wheel will approach a certain average temperature and periodic fluctuations around this temperature will occur.

The conventional theory for calculation of the heat transfer coefficient in rotating regenerative heat exchangers was established in the 1930s by Hausen. The following equation is given for U:

$$\frac{1}{U} = (\tau_1 + \tau_2)\left(\frac{1}{\alpha_1\tau_1} + \frac{\delta_m}{3\lambda_m}\left(\frac{1}{\tau_1} + \frac{1}{\tau_2}\right) + \frac{1}{\alpha_2\tau_2}\right) \tag{58}$$

where τ_1 and τ_2 are the time durations the matrix is in contact with fluids 1 and 2, respectively. The parameter δ_m is the material thickness and λ_m is its thermal conductivity. The parameters α_1 and α_2 are the heat transfer coefficients in the channels for fluids 1 and 2, respectively.

The analysis by Hausen was based on several assumptions and later research has suggested other methods for the analysis.

Reference 28 gives the following method to analyze a rotating regenerator in counterflow:

$$\varepsilon = \varepsilon_{\text{counterflow}} \times \left[1 - \frac{1}{9(C_r^*)^{1.93}}\right] \tag{59}$$

where $\varepsilon_{\text{counterflow}}$ is the effectiveness of a nonrotating counterflow heat exchanger and

$$C_r^* = \frac{(mc_p)_{\text{heat exchanger}}\omega}{C_c} \tag{60}$$

$(mc_p)_{\text{heat exchanger}}$ is the heat capacity of the matrix material, ω the rotational speed [revolutions/s] and $C_c = (\dot{m}c_p)_{\text{cold fluid}}$.

If the heat capacity flow rates of the hot and cold fluids are equal, ie, $C_c = C_h$, one has (see Table 7)

$$\varepsilon = \frac{\text{NTU}_0}{1 + \text{NTU}_0} \times \left[1 - \frac{1}{9(C_r^*)^{1.93}}\right] \tag{61}$$

where

$$\text{NTU}_0 = \frac{1}{C_{\min}}\left[\frac{1}{(1/\alpha A)_c + (1/\alpha A)_h}\right] \tag{62}$$

For heat exchangers of material with high thermal conductivity, a correction due to longitudinal heat conduction must be introduced. One then has

$$\varepsilon = \varepsilon \times \text{correction}_\lambda \tag{63}$$

Reference 28 gives when $C_c = C_h$

$$\text{correction}_\lambda = 1 - \left[\frac{1}{1 + \text{NTU}_0 \frac{(1+\lambda\Phi)}{(1+\lambda\text{NTU}_0)}} - \frac{1}{1 + \text{NTU}_0}\right] \tag{64}$$

where $\lambda = \left[\frac{\lambda_{\text{heat exchanger}} A_{\text{vl}}}{LC_{\min}}\right]$, $\lambda_{\text{heat exchanger}}$ is the thermal conductivity of the heat exchanger material, A_{vl} is the heat conducting area in the longitudinal direction, and

$$\Phi \approx \sqrt{\frac{\lambda\text{NTU}_0}{1 + \lambda\text{NTU}_0}}$$

3.12. Frictional Pressure Drop. In the description of calculation methods for the pressure drop in compact heat exchangers and shell-and-tube heat exchangers, the frictional pressure drop appeared. The frictional pressure drop inside a heat exchanger results when fluid particles move at different velocities because of the presence of structural walls, eg, tubes, shell, and channels. It is calculated from a well-known expression as

$$(\Delta p)_{\text{friction}} = f_{\text{D}} \frac{L}{D_h} \left(\frac{1}{2} \rho V^2 \right) \tag{65}$$

where f_{D} is the Darcy friction factor $= 4f$, and f is the Fanning friction factor; D_h is the hydraulic or equivalent diameter $=$ 4(flow area)/(flow perimeter); and ½ ρV^2 is the dynamic pressure. The Darcy friction factor, f_{D}, can be derived from a theoretical analysis of fluid flow in a closed conduit; for laminar flow

$$f_{\text{D}} = \frac{64}{Re} \tag{66}$$

and for turbulent flow

$$f_{\text{D}} = \frac{0.184}{Re^{0.2}} \tag{67}$$

Equation 67 is applicable to smooth-walled conduits for $10,000 < Re < 120,000$. In general, f_{D} is a function of the Reynolds number, Re, and the relative roughness of conduit surface, ε_w/D_h, as shown in the Moody diagram, Figure 40.

Pressure Drop from Area Change. Pressure drop from area change occurs as a result of energy dissipation associated with eddies formed when a flow area is suddenly expanded or contracted. It is expressed in the following form:

$$(\Delta p)_{\text{area change}} = K \left(\frac{1}{2} \rho V_{\text{max}}^2 \right) \tag{68}$$

where K is the pressure loss coefficient and V_{max} is the flow velocity based on smaller or minimum flow area. The parameter K is a function of flow/area ratio and is given in Figure 41 for both sudden contraction and expansion cases. Equation 76 may be used to calculate pressure drops from inlet nozzles to shell or channel, from shell or channel to outlet nozzles, and tube side inlet and exit losses. When there is a gradual change in tube diameter, the corresponding pressure-loss coefficient can be determined using the curve given in Figure 41**c**.

Pressure Drop Owing to Flow Turning. When a fluid turns along a curved surface or mitered bend, a secondary flow is formed as a result of centrifugal force acting on fluid particles. An energy dissipation follows, and the pressure decreases. The pressure drop associated with flow turning is expressed as

$$(\Delta p)_{\text{turning}} = K \left(\frac{1}{2} \rho V^2 \right) = f_{\text{D}} \left(\frac{L}{D_h} \right)_{\text{equivalent}} \left(\frac{1}{2} \rho V^2 \right) \tag{69}$$

where K is the turning-loss coefficient (see Fig. 42), V is the flow velocity calculated based on the upstream unaffected flow area, and L/D_h is an equivalent length/diameter ratio. The equivalent length/diameter ratio concept can also be used in conjunction with a familiar friction pressure-drop formula of equation. The pressure drops in a U-bend section of U-tubes in a heat exchanger can be calculated using a similar approach as given in equation 69.

3.13. Special Applications. *High Temperature and Waste Heat Recovery Exchangers.* Heat exchangers in industrial process heating applications are commonly used to improve process efficiency by preheating the combustion air using waste heat from the flue gases. Advances in these heat exchangers should have significant impact on energy savings in primary metal, glass, and ceramic firing industries.

The primary need in the development of heat exchangers for recuperation in high temperature industrial processes does not relate mainly to heat transfer issues but rather to material durability. Heat exchangers need to withstand high temperatures and corrosiveness of gases, eg, those containing sodium silicates and chlorine and potassium salts. To date no low cost ceramic materials are available for heat exchangers for these conditions. In addition, because these ceramic components must be mated to metallic components, methods to obtain ceramic-to-metallic seals must be obtained to simplify manufacturing and installation of recuperation equipment in these applications. Moreover, the autoregenerative burners are expensive; thus, new burners that produce low NO_x and are reasonable in price should be developed. There is good potential for the application of low cost, easily retrofitted passive heat transfer enhancement techniques to high temperature waste heat recovery, as well as to high temperature process heat exchangers/reactors, eg, fired heaters, steam reformers, and other process vessels used in the petrochemical industries. A better understanding of the radiative properties of exhaust gas streams would allow better design of such heat exchangers.

Low Temperature Difference Heat Exchangers. Many applications exist in which the extraction of thermal energy from low temperature differences between the source and sink is discussed. Some examples are ventilation applications, ocean thermal energy conversion (OTEC) power plants, and atmosphere thermal energy conversion (ATEC) power plants to recover thermal energy owing to a temperature difference between a mountaintop and the valley. In the latter two examples, abundant free energy can be harnessed if the appropriate inexpensive durable heat exchangers are available. These low temperature difference heat exchangers would require very large areas. This is the principal disadvantage and limitation.

The success of low temperature difference applications depends on the development of special inexpensive materials, heat-exchanger constructions, and surfaces having high heat transfer performance at a very low pressure drop, ie, low pumping power requirements. Whereas low cost paper and plastic exchangers are commercially available for ventilation applications, specialized materials and exchanger constructions are needed to provide cost-effective exchangers with durability and good performance. The OTEC power plants have not materialized because heat-exchanger capital and operating costs are too high, and the life is too short.

Direct Contact Heat Exchangers. In a direct contact exchanger, two fluid streams come into direct contact, exchange heat, and possibly mass, and then separate. Very high heat transfer rates, practically no fouling, lower capital costs, and lower approach temperatures are the principal advantages.

Cooling towers are excellent examples of direct contact heat exchangers. Sparging, ie, a process of forcing gas or water vapor through liquid to remove undesirable gases using low pressure steam, is a common way to heat up material in the food industry. When chemical reactions must be stopped very quickly,

direct quenching downstream of the reactor is often employed. Beds of solids are often heated by direct contact with fluidizing gas, eg, in fluidized-bed dryers.

Direct contact heat exchangers have, however, received limited use in conventional power and process applications. These exchangers appear to offer advantages in some geothermal power applications and have been proposed for use in ocean thermal energy conversion-system designs. Direct contact heat transfer also plays an important role in some nuclear accident scenarios in which vapor produced in an accident is condensed by bringing it into direct contact with colder water. Applications of direct contact exchanger technology could come in the biotechnology area, where direct contact heat transfer/mass transfer/reactor units may be used in the production and processing operations in genetic engineering technology. Whereas the uses of direct contact exchanger technology are not completely understood, the potential impact could be great, particularly in aerospace power and heat-exchanger designs.

Heat Exchangers Using Non-Newtonian Fluids. Most fluids used in the chemical, pharmaceutical, food, and biomedical industries can be classified as non-Newtonian, ie, the viscosity varies with shear rate at a given temperature. In contrast, Newtonian fluids, eg, water, air, and glycerin, have constant viscosities at a given temperature. Examples of non-Newtonian fluids include molten polymer, aqueous polymer solutions, slurries, a coal–water mixture, tomato ketchup, soup, mayonnaise, purees, suspension of small particles, blood, etc. Because non-Newtonian fluids are nonlinear in nature, these are seldom amenable to analysis by classical mathematical techniques.

The optimum design of process equipment that handles non-Newtonian fluids could be significantly improved once predictive capability were increased. However, the basic understanding of the fluid mechanical and heat transfer behavior of non-Newtonian, ie, viscous and viscoelastic, fluids, is limited. A better understanding of pressure drop and heat transfer behavior of non-Newtonian flows applicable to typical heat-exchanger geometries should lead to the design and development of more energy-efficient processes and to better quality control of the final products. In general, the viscosity of a non-Newtonian fluid can be significantly larger than that of water. Therefore, the selection of a pump size to provide enough flow rate and subsequently to ensure adequate heat removal or supply is necessary.

A significant heat transfer enhancement can be obtained when a noncircular tube is used together with a non-Newtonian fluid. This heat transfer enhancement is attributed to both the secondary flow at the corner of the noncircular tube and to the temperature-dependent non-Newtonian viscosity. By using an aqueous solution of polyacrylamide, the laminar heat transfer can be increased by $\sim$300% in a rectangular duct over the value of water. For further details, see References 31–33.

A knowledge of the viscous and thermal properties of non-Newtonian fluids is essential before the results of the analyses can be used for practical design purposes. Because of the nonlinear nature, the prediction of these properties from kinetic theories is in its infancy. For the purpose of design and performance calculations, physical properties of non-Newtonian fluids must be measured.

Microheat Exchangers. A better understanding of transport phenomena in microchannel heat exchangers appears to be vital to the development of some advanced microelectronic devices. In future designs, heat-exchanger passages

are expected to be incorporated into silicon substrates for the purpose of cooling substrate-mounted microelectronic chips. The passage dimensions could be made as small as those of the chip features, in which case the passage size may be comparable to the mean free path of air molecules pumped through the passages. The spacing between two molecules of gas is on the order of 1 μm, whereas that of liquid is on the order of 0.1 μm.

For further research on convective transport under low Reynolds number, quasicontinuum conditions is needed before the optimal design of such a microheat exchanger is possible. The cooling heat exchanger is usually thermally linked to a relatively massive substrate. The effects of this linkage need to be explored and accurate methods of predicting the heat transfer and pressure-drop performance need to be developed.

Electrohydrodynamic-Based Heat Exchangers. Electrohydrodynamics refers to the coupling of an electric and velocity field in a dielectric fluid continuum. Electric field effects on heat transfer in polar gases generally take place via a modification of the gas velocity and temperature boundary layers. Electric fields in complex flows act to change the character of flow stability. Applications of electrohydrodynamics in convective heat transfer are diverse, eg, in heating ventilation or air conditioning (HVAC) cooling of electronic equipment applications, space power applications, micromachines, ultrasmall high duty heat exchangers, and noninvasive flow control techniques.

Characterization and influence of electrohydrodynamic secondary flows on convective flows of polar gases is lacking for most simple, as well as complex, flow geometries. Such investigations should lead to an understanding of flow control, manipulation of separating, and accurate computation of local heat transfer coefficients in confined, complex geometries. The typical Reynolds number of the bulk flow does not exceed 5000.

3.14. Special Topics. *Flow-Induced Vibrations.* One of the critical limitations of the increased performance of shell-and-tube heat exchangers is the onset of flow-induced vibrations at high shell side fluid flows that result in a loud acoustic (noise) vibration of >150 dB, or the vibration of tubes to the extent that the tube walls are worn through. Whereas a great deal of research has been done to understand vibration excitation mechanisms and to develop design guides, much is unknown about predicting flow-induced vibration occurrence, the location and type of damage, and the rates of wear. There is a substantial dependence on experience with the hardware in service, and this severely limits the development of the next generation of heat exchangers. Elimination or substantial minimization of flow-induced vibrations would have a significant impact in power, process, petroleum, and other industries that use shell-and-tube exchangers (34).

Flow Maldistribution. One of the principal reasons for heat exchangers failing to achieve the expected thermal performance is that the fluid flow does not follow the idealized anticipated paths from elementary considerations. This problem is referred to as a flow maldistribution. As much as 50% of the fluid can behave differently from what is expected based on a simplistic model (35), resulting in a significant reduction in heat-transfer performance, especially at high NTU or a significant increase in pressure drop. Flow maldistribution is the main culprit for reduced performance of many heat exchangers.

In addition to the reduction in performance, flow maldistribution may result in increased corrosion, erosion, wear, fouling, fatigue, and material failure, particularly for liquid flows. This problem is even more pronounced for multiphase or phase change flows as compared to single-phase flows. Flow distribution problems exist for almost all types of exchangers and can have a significant impact on energy, environment, material, and cost in most industries.

For gross flow maldistribution in heat exchangers, modeling is available for heat transfer performance prediction, but no modeling is available for pressure-drop prediction. The reason is because, in most of the cases, the static pressure distribution is not uniform at the exchanger inlet and outlet faces, and no modeling or computational fluid dynamic analysis is possible without the boundary conditions. Gross flow maldistribution significantly increases pressure drop. In addition, because there are an infinite number of gross flow maldistributions possible, the only approach is to analyze the problem numerically for idealized uniform pressure boundary conditions.

No systematic study is reported to quantify the effect of manifold induced-flow maldistribution on a single-phase pressure drop and heat transfer in a heat exchanger. Such flow maldistribution is common in gas-to-gas and liquid-to-gas exchangers with manifolds, and in a plate heat exchanger where many parallel passages are connected by inlet and outlet pipe manifolds created by plate ports. For two-phase flow distribution, however, no practical methods exist for ensuring the adequate distribution of the vapor and liquid phases among many parallel-flow channels. The result in the cryogenic gas processing area is, eg, that phases are separated and introduced into separate heat exchangers for further vaporization or condensation at a significant penalty in overall thermodynamic optimization of the system. Viscosity-induced flow maldistribution has been hardly analyzed to quantify the influence on heat transfer and pressure drop. Very meager information is available in the literature on natural convection-induced flow maldistribution and its effect on the exchanger heat transfer and pressure drop. A combination of hot- and cold-fluid maldistributions, both tube side and shell side, can create a more serious problem than the individual maldistributions alone. Heat exchangers involving multiphase flow appear to have the highest likelihood of flow maldistribution and the resulting thermal and mechanical performance loss and flow instability. This is especially critical where multiphases exist at inlet.

Recent investigations are exemplified by References 36, 37.

Header Design. Headers, ie, manifolds and tanks, are the chambers or transition ducts at each end of the heat-exchanger core on each fluid side for distributing fluid to the core at the inlet and collecting fluid at the exit. These may be classified broadly as normal, turning, and oblique flow headers. Poor design of headers reduces heat transfer performance significantly and may also increase pressure drop substantially owing to flow maldistribution, flow separation, and jet effects. Thus header design is an important problem for all heat exchangers where fluid from the inlet pipe is distributed to the exchanger core via manifolds and tanks. If novel heat-exchanger applications are contemplated, the header volume must be a very small fraction of the total exchanger volume, particularly for highly compact heat-exchanger applications.

No design theory and modeling is available to obtain uniform flow for normal headers, ie, diffusers having downstream flow resistance and turning headers, with or without vanes. Only very limited design information is available for oblique flow headers. Manifolds in a heat exchanger can be further classified into four types: dividing, combining, parallel, and reverse flow manifolds. Parallel and reverse flow manifolds are those that combine dividing and combining flow manifolds. In a parallel flow manifold, the flow directions in dividing and combining flow headers are the same; in a reverse flow manifold, the flow directions are opposite. The objective of the manifold design is to obtain a uniform flow distribution in the heat-exchanger core, with the manifold occupying the smallest fraction of volume of the total heat exchanger.

Most experimental studies on manifolds are limited to turbulent flow in circular pipes. The flow characteristics of branch points in manifolds and the effect of the Reynolds number and branch pipe resistance on the flow distribution in dividing and combining flow manifolds have been studied using water. In the latter case, the branch pipe resistance was varied by using different size orifice plates. The flow distribution, which was independent of the Reynolds number in a range of $Re = 30{,}000–100{,}000$, was found to improve with the increase of branch pipe resistance. Reverse and parallel flow manifolds have been studied both analytically and experimentally using hair. A manifold having a smaller area ratio (AR = 1.41) had a better flow distribution than the one having a larger area ratio (AR = 2.81), regardless of the resistance in branch pipes. The area ratio, AR, is the ratio of the total channel cross-sectional area to the dividing flow header cross-sectional area. Several investigations have also been conducted using analytical and numerical approaches on dividing and combining flow manifolds.

Material Selection. For most heat exchangers, the material selection and the manufacture are quite distinct. These are further dependent upon the specific application and so, eg, the heat duty, type of fluids being handled, and mode of heat transfer (single-phase flows, boiling, and condensation) are important. With respect to corrosion, the compatibility between the construction materials and working fluids is essential and thus the corrosiveness of the working fluid might be a selection criterion. Other criteria might be fouling and erosion. The properties of the required material, however, seldom affect the design that can be used.

For PHE stainless steels, nickel alloys, titanium, and titanium alloys are common, but there are also others, eg, graphite, copper and copper alloys, tantalum, and aluminum appear. For gasketed plate-and-frame heat exchangers, the gasket material is also very important. This is selected according to the operating conditions, eg, fluid type, concentration, and temperature, and has a direct influence on lifetime, reliability and safety. Gaskets are commonly made of various elastic and formable materials, eg, rubber. Further details can be found in Refernece 38.

Shell-and-tube heat exchangers can be designed using a variety of materials, both metallic and nonmetallic. If carbon steel can be used, the heat exchanger can be manufactured cheaply. More information is available in Reference 39. Compact heat exchangers have to satisfy requirements on low cost, light weight, ease of manufacturing, high thermal conductivity, and where applicable aluminum is often selected.

4. Nomenclature

Symbol	Parameter	Units
A	heat transfer surface area, flow area	m^2
AR	area ratio	
a	thermal diffusivity	m^2/s
b	thickness	m
C	heat capacity flow rate	W/K
C_R	ratio of $C_{\min}$ to $C_{\max}$	
C_r^*	heat capacity ratio rotating heat exchanger	
c_p	specific heat at constant pressure	J/kgK
D	diameter	m
D_c, D_d	width of combining and dividing flow headers	m
D_h	hydraulic or equivalent diameter	m
E_B	emissive power	W/m^2
F	LMTD correction factor	
F_{ik}	view factor between surfaces i and k	
f	Fanning friction factor	
f_D	Darcy friction factor	
G	mass flux	kg/m^2s
h	heat transfer coefficient	W/m^2K
J	radiosity	W/m^2
K	pressure loss coefficient	
k	thermal conductivity	W/mK
L	length or manifold length	m
LMTD	logarithmic mean temperature difference	K
m	fin parameter or exponent	1/m
$\dot{m}$	mass flow rate	kg/s
N	number of tube rows traversed by fluid	
Nu	Nusselt number	
Nu_{H2}	Nusselt number for uniform wall heat flux boundary condition	
Nu_T	Nussellt number isothermal wall boundary condition	
NTU	number of transfer units	
n	number of shells or exponent	
P	temperature efficiency	
P_m	perimeter or circumference	m
Pr	Prandtl number	
p_f	fin pitch	m
p	pressure	N/m^2
$\dot{Q}$	heat transfer rate	W
q	heat flux	W/m^2
R	ratio of heat capacity flow rates	
Re	Reynolds number	
r	radius	m
St	Stanton number	
S_t	transverse tube pitch	m

S_l	longitudinal tube pitch	m
s	open space between fins	m
TR	thermal resistance	K/W
t	temperature or thickness	K, m
U	overall heat transfer coefficient	W/m^2K
u_m	mean flow velocity	m/s
V	flow velocity	m/s
x	length	m
Greek symbols		
α	heat transfer coefficient	W/m^2K
$1/\alpha_F$	fouling factor	m^2K/W
ΔA	additional surface area	m^2
Δp	pressure difference or drop	N/m^2
Δt	temperature difference	K
Δt_m	mean temperature difference	K
δ	thickness	m
ε	heat exchanger effectiveness, emissivity	
ε_w	surface roughness	m
θ	thermal length	
λ	thermal conductivity	W/mK
μ	dynamic viscosity	kg/ms
ν	kinematic viscosity	m^2/s
ρ	density	kg/m^3
σ	area ratio	
τ	time	s
φ	fin efficiency	
φ_o	total fin efficiency	
Subscripts		
b	base of fin	
c	cold or heated fluid, cross flow	
d	diameter	
eff	effective	
f	fin, fouling, fluid, front	
h	hot or heating fluid	
i	inside	
in	inlet	
max	maximum	
min	minimum	
o	outside	
out	outlet	
s	shell side	
t	tube side	
w	wall, window	
x	flow length direction	
∞	at far distances	

BIBLIOGRAPHY

"Heat Transfer" in *ECT* 1st ed., Vol. 7, pp. 370–389, by G. T. Skaperdas, The M. W. Kellogg Co.; in *ECT* 2nd ed., Vol. 10, pp. 819–846, by G. T. Skaperdas, The M. W. Kellogg Co., Division of Pullman Inc.; "Heat Transfer" under "Heat Exchange Technology" in *ECT* 3rd ed., Vol. 12, pp. 129–170, by J. P. Fanaritis, J. A. Kwas, and A. T. Chase, Struthers Wells Corp.; "Heat Transfer" under "Heat-Exchange Technology" in *ECT* 4th ed., Vol. 12, pp. 950–990, by Y. I. Cho, Drexel University, and S. M. Cho, Foster Wheeler Energy Corp.; "Heat-Exchange Technology, Heat Transfer" in *ECT* (online), posting date: December 4, 2000, by Y. I. Cho, Drexel University, and S. M. Cho, Foster Wheeler Energy Corp.; "Heat Transfer" in *ECT* 5th ed., Vol. 13, pp. 242–281, by Y. I. Cho, Drexel University, and S. M. Cho, Foster Wheeler Energy Corp.

CITED PUBLICATIONS

1. F. P. Incropera and D. P. DeWitt, *Fundamentals of Heat and Mass Transfer*, 5th ed., John Wiley & Sons, Inc., New York, 2002.
2. J. P. Holman, *Heat Transfer*, 9th ed., McGraw-Hill, New York, 2002.
3. G. Walker, *Industrial Heat Exchangers: A Basic Guide*, 2nd ed., Hemisphere Publishing Corp., New York, 1990.
4. M. N. Özisik, *Heat Transfer—A Basic Approach*, McGraw-Hill, New York, 1985.
5. *Tubular Exchanger Manufacturers Association*, Standards, TEMA, New York, 1959.
6. E. F. C. Somerscales and J. G. Knudsen, *Fouling of Heat Transfer Equipment*, Hemisphere Publishing Corp., Washington, D.C., 1980.
7. N. Epstein, Fouling in heat exchangers, *Proceeding of the 6th International Heat Transfer Conference*, Vol. 6, Toronto, 1978, pp. 235–253,.
8. N. Epstein, Fouling in heat exchangers and fouling: Technical aspects, in E. F. C. Somerscales and J. G. Knudsen, eds., *Fouling of Heat Transfer Equipment*, Hemisphere Publishing Corp., New York, 1981, pp. 701–734, 31–53.
9. R. A. Bowman, A. C. Mueller, and W. M. Nagle, *Trans. ASME*, **62**, 283, (1940).
10. K. A. Gardner, *Trans. ASME*, **67**, 31 (1945).
11. R. A. Stevens, J. Fernandes, and J. R. Woolf, *Trans. ASME*, **79**, 287, (1957).
12. *Heat Exchangers Design Handbook*, Hemisphere Publishing Corp., Washington, D.C., 1983.
13. W. M. Kays and A. L. London, *Compact Heat Exchangers*, 3rd ed., McGraw-Hill, New York, 1984.
14. D. Eriksson and B. Sundén, Plate fin-and-tube heat exchangers: A literature survey of heat transfer and friction correlations, in B. Grochal, J. Mikielewicz, and B. Sundén, eds., *Progress in Engineering Heat Transfer*, IFFM Publishers, Gdansk Poland, 1999, 533–540.
15. L. Gray and R. L. Webb, Heat transfer and friction factor for plate finned-tube heat exchangers, *Proceeding 9th Internationl Heat Transfer Conference*, Vol. 6, 1986, pp. 2745–2750.
16. A. Zukauskas, *High-Performance Single-Phase Heat Exchangers*, Hemisphere Publihsing Corp., Washington, D.C., 1989.
17. R. L. Webb and N. H. Kim, *Principles of Enhanced Heat Transfer*, 2nd ed., Taylor & Francis, Pennsylvania, Pa., 2005.
18. R. L. Webb, Enhancement of single-phase heat transfer, Chapt. 17, in S. Kakac, R. K. Shah, and W. Aung, eds., *Handbook of Single-Phase Convective Heat Transfer*, John Wiley & Sons,Inc., New York, 1987.

19. B. Sundén and I. Karlsson, *Exp. Ther. Fluid Sci.*, **4**(3), 305 (1991).
20. B. Sundén and J. Svantesson, Thermal hydraulic performance of new multi-louvered fins, in *Heat Transfer 1990*, G. Hetsroni, ed., Vol. 5, Hemisphere Publishing Corp., New York, 1990, pp. 92–96.
21. B. Sundén, and J. Svantesson, *Exp. Heat Transfer* **4**, 111 (1991).
22. A. Achaichia and T. A. Cowell, *Exp. Thermal Fluid Sci.*, **1**, 147, (1988).
23. T. Tinker, Shell side characteristics of shell and tube heat exchangers, *Proceedings General Discussions on Heat Transfer*, Institute Mechenical Engineering, London, 1951.
24. A. Zukauskas, Heat transfer from tubes in cross flow, *Advances in Heat Transfer*, Vol. 18, Academic Press, New York, 1987, pp. 87–159.
25. A. Zukauskas and R. Ulinskas, *Heat Transfer in Tube Banks in Cross Flow*, Hemisphere Publishing Corp., New York, 1988.
26. A. Zukauskas, V. Katinas, and R. Ulinskas, *Fluid Dynamics and Flow Induced Vibration of Tube Banks*, Hemisphere Publishing Corp., New York, 1988.
27. S. S. Chen, *Flow-Induced Vibration of Circular Cylindrical Structures*, Hemisphere Publishing Corp., New York, 1987.
28. W. M. Rohsenow, J. P. Hartnett, and E. N. Ganic, *Handbook of Heat Transfer: Applications*, 2nd ed., McGraw-Hill, New York, 1985.
29. B. R. Munson, D. F. Young, and T. H. Okiishi, *Fundamentals of Fluid Mechanics*, 5th ed., John Wiley & Sons, Inc., New York, 2006.
30. F. M. White, *Fluid Mechanics*, 5th ed., McGraw-Hill, New York, 2003.
31. J. P. Hartnett and M. Kostic, *Int. J. Heat Mass Transfer*, **28**, 1147 (1985).
32. C. Xie and J. P. Hartnett, *Int. J. Heat Mass Transfer* **35**, 641 (1992).
33. S. Shin, W. K. Gingrich, Y. I. Cho, and W. Shyy, *Int. J. Heat Mass Transfer* **36**, 4365 (1993).
34. R. D. Blevins, *Flow-Induced Vibration*, Van Nostrand Reinhold, New York, 1990.
35. E. A. D. Saunders, *Heat Exchangers: Selection, Design and Construction*, John Wiley & Sons, Inc., New York, (1988).
36. B. P. Rao, B. Sunden, and S. K. Das, *ASME J. Heat Transfer*, **127**, 332 (2005).
37. P. R. Bobbili, B. Sunden, and S. K. Das, *Appl. Thermal Eng.*, **26**, 1919 (2006).
38. L. Wang, R. M. Manglik, and B. Sunden, *Plate heat exchangers: Design, Applications and performance*, WIT Press, 2007.
39. *Heat Exchanger Design Handbook*, Hemsisphere Publishing Corp., New York, 1983.

Additional References

B. Sunden and M. Faghri, *Computer Simulations in Compact Heat Exchangers*, Computational Mechanics Publications U. K., 1998.
B. Sunden and P. J. Heggs, *Recent Advances in Analysis of Heat Transfer for Fin Type Surfaces*, WIT Press, Southampton, U.K., 1999.
E. M. Smith, *Thermal Design of Heat Exchangers—A Numerical Approach*, John Wiley & Sons, Inc., New York, 1997.
A. D. Kraus, A. Aziz, and J. R. Welty, *Extended Surface Heat Transfer*, John Wiley & Sons, Inc., New York, 2001.
J. E. Hesselgreaves, *Compact Heat Exchangers—Selection, Design and Operation*, Pergamon Press, U.K., 2001.
R. K. Shah and D. P. Sekulic, *Fundamentals of Heat Exchanger Design*, John Wiley & Sons, Inc. New York, 2003.

G. F. Hewitt, G. L. Shires, and T. R. Bott, *Process Heat Transfer*, CRC Press, Boca Raton, Fla., 1994.
G. F. Hewitt, G. L. Shires, and Y. V. Polezhaev, *International Encyclopedia of Heat and Mass Transfer*, CRC Press, Boca Raton, Fla., 1997.

BENGT SUNDEN
Lund University

Table 1. **Thermal Conductivity for Some Materials**

	Thermal conductivity, W/mK			
Material	at 20°C	at 100°C	at 300°C	Specific heat at 20°C, kJ/kgK
aluminium	204	206	228	896
carbon steel, 1.0%	43	43	40	473
copper	386	379	369	381
brass, Cu 85%, Zn 30%	111	128	147	385
stainless steel, AISI304	14.9	17	19	477
water	0.613	0.683		4239
air	0.0261	0.0331	0.0456	1014

Table 2. **Typical Values of the Convective Heat Transfer Coefficient**

Material	Convection process	W/m^2K	$Btu/(h,ft^2\ ^\circ F)$
air	free, natural	2–25	0.4–5
air	forced	25–250	5–50
water	free, natural	50–1,000	10–200
water	forced	50–20,000	10–4,000
water	boiling	2,500–100,000	500–20,000
water vapor	condensing	5,000–100,000	1,000–20,000

Table 3. **Correlations for Convective Heat Transfer, Circular Tube Flow (1, 2)**

Fully developed flow	Nu_d	Pr
Laminar	4.364^a, 3.656^b	
turbulent, smooth tube		
$Re_d \geq 10{,}000^c$	$0.027\, Re_d^{0.8}\, Pr^{1/3}\, (\mu/\mu_w)^{0.14}$	$0.7 \leq Pr < 16,700$
$Re_d \leq 20{,}000$		$0.6 \leq Pr < 160$
$Re \geq 20{,}000$	$0.023\, Re_d^{0.8} Pr^{n^d}$	$0.6 \leq Pr < 160$

[a]Constant wall heat flux.
[b]Constant wall temperature.
[c]For temperature-dependent viscosity.
[d]$n = 0.4$ for heating, $n = 0.3$ for cooling.

Table 4. **Correlations for Convective Heat Transfer for External Flow (1,2)**

laminar flow surface	Nusselt number	Re_d	C	m
flat plate, where $0.6 \leq Pr \leq 50$[a]	$0.664 Re_x^{0.5} Pr^{1/3}$			
circular cylinder, where $0.4 \leq Re_d \leq 400{,}000$[b]	$C Re_d^m Pr^{1/3}$	1–40	0.75	0.4
		40–1000	0.51	0.5
		1×10^3–2×10^5	0.26	0.6
		2×10^5–10^6	0.076	0.7

[a] $Nu_{x,\ \mathrm{avg}}$.
[b] Nu_d.

Table 5. **Correlations for Heat Transfer Coefficients for Noncircular Laminar Duct Flow (1, 2)**

Duct design	Nu_{H2}[a]	Nu_T[b]
square	3.091	2.976
rectangular, aspect ratio		
0.5	3.017	3.391
0.25	4.35	3.66
triangular, isosceles	1.892	2.47

[a] Nu_{H2} is the Nusselt number for uniform heat flux boundary condition along the flow direction and periphery.
[b] Nu_T is the Nusselt number for uniform wall temperature boundary condition.

Table 6. **Fouling Factors**

Fluid	$1/\alpha_F$, m^2K/W
destilled water	1×10^{-4}
seawater ($T < 325$ K)	1×10^{-4}
seawater ($T > 325$ K)	2×10^{-4}
feed water to furnaces	2×10^{-4}
oil	9×10^{-4}
dirty air	3.5×10^{-4}

Table 7. **ε-NTU Relations for Some Common Heat Exchanger Types (HEX)**

HEX-type[a]	ε^a	Figure
parallel flow	$\varepsilon = \dfrac{1-\exp[-\mathrm{NTU}(1+C)]}{1+C}$	25**b**
counter flow	$\varepsilon = \dfrac{1-\exp[-\mathrm{NTU}(1-C)]}{1-C\exp[-\mathrm{NTU}(1-C)]} \quad C<1$	25**a**
	$\varepsilon = \dfrac{\mathrm{NTU}}{1+\mathrm{NTU}} \quad C=1$	
(shell-and-tube HEX)		
1 Shell pass 2,4,6,..., tube passes	$\varepsilon_1 = 2\left\{1+C+(1+C^2)^{1/2} \times \dfrac{1+\exp\left[\dfrac{-\mathrm{NTU}(1+C^2)^{1/2}}{-\mathrm{NTU}(1+\mathrm{C}^2)^{1/2}}\right]}{1-\exp}\right\}^{-1}$	26**a**
n Shell passes $2n$, $4n$,..., tube passes	$\varepsilon_n = \left[\left(\dfrac{1-\varepsilon_1 C}{1-\varepsilon_1}\right)^n - 1\right]\left[\left(\dfrac{1-\varepsilon_1 C}{1-\varepsilon_1}\right)^n - C\right]^{-1}$	26**b**
cross-flow (single pass)		
both fluids unmixed	$\varepsilon \approx 1-\exp[C^{-1}(\mathrm{NTU})^{0.22}\{\exp[-C(\mathrm{NTU})^{0.78}]-1\}]$	26**c**
both fluids mixed	$\varepsilon = \mathrm{NTU}\left[\dfrac{\mathrm{NTU}}{1-\exp(-\mathrm{NTU})} + \dfrac{C(\mathrm{NTU})}{1-\exp[-C(\mathrm{NTU})]} - 1\right]^{-1}$	26**d**
$C_{\min}$ unmixed $C_{\max}$ mixed	$\varepsilon = C^{-1}(1-\exp[-C\{1-\exp(-\mathrm{NTU})\}])$	26**f**
$C_{\min}$ mixed $C_{\max}$ unmixed	$\varepsilon = 1-\exp(-C^{-1}\{1-\exp[-C(\mathrm{NTU})]\})$	26**e**
All heat exchangers $C=0$	$\varepsilon = 1-\exp(-\mathrm{NTU})$	

[a] $C = C_{\min}/C_{\max}$.

Table 8. **ε-NTU Relations for Some Common Heat Exchangers (HEX)**

HEX-type[a]	NTU[a]	Figure
parallel flow	$\mathrm{NTU} = -\dfrac{\ln[1-\varepsilon(1+C)]}{1+C}$	**25b**
counterflow **(shell-and-tube HEX)**	$\mathrm{NTU} = \dfrac{1}{C-1}\ln\left(\dfrac{\varepsilon-1}{\varepsilon C-1}\right) \quad C<1$ $\mathrm{NTU} = \dfrac{\varepsilon}{1-\varepsilon} \quad C=1$	**25a**
1 shell pass 2,4,6,..tube passes	$\mathrm{NTU} = -(1+C^2)^{-1/2}\ln\left(\dfrac{E-1}{E-1}\right)$ $E = \dfrac{2/\varepsilon_1-(1+C)}{(1+C^2)^{1/2}}$	**26a**
n shell passes $2n$, $4n$,... tube passes	Use the expression for one shell pass but with $\varepsilon_1 = \dfrac{F-1}{F-C}$ where $F = \left(\dfrac{\varepsilon C-1}{\varepsilon-1}\right)^{1/n}$	**26b**
cross-flow (one pass)		
$C_{\min}$ unmixed $C_{\max}$ mixed	$\mathrm{NTU} = -\ln[1+C^{-1}\ln(1-\varepsilon C)]$	**26f**
$C_{\min}$ mixed $C_{\max}$ unmixed	$\mathrm{NTU} = -C^{-1}\ln[C\ln(1-\varepsilon)+1]$	**26e**
all heat exchangers $C = 0$	$\mathrm{NTU} = -\ln(1-\varepsilon)$	

[a] $C = C_{\min}/C_{\max}$.

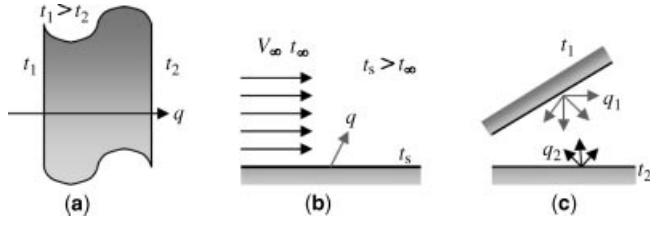

Fig. 1. Heat transfer by (**a**) heat conduction, (**b**) convection, (**c**) thermal radiation.

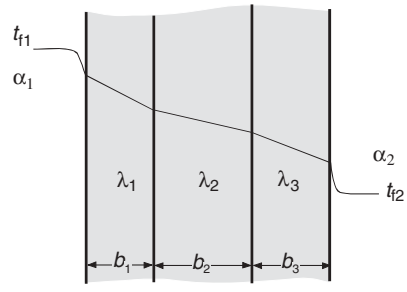

Fig. 2. Heat flow through a composite wall with convective heating and cooling.

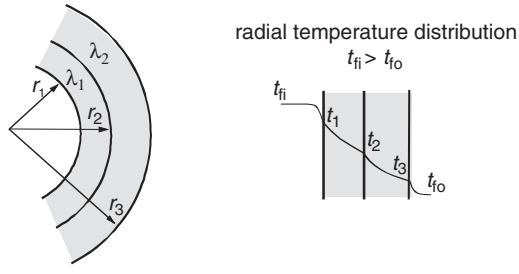

Fig. 3. A composite tube wall with internal and external convection.

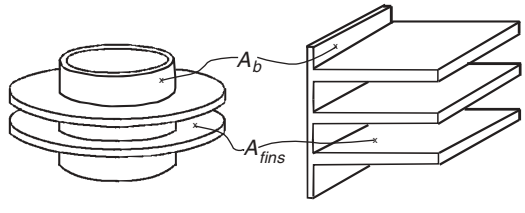

Fig. 4. Typical fin configurations.

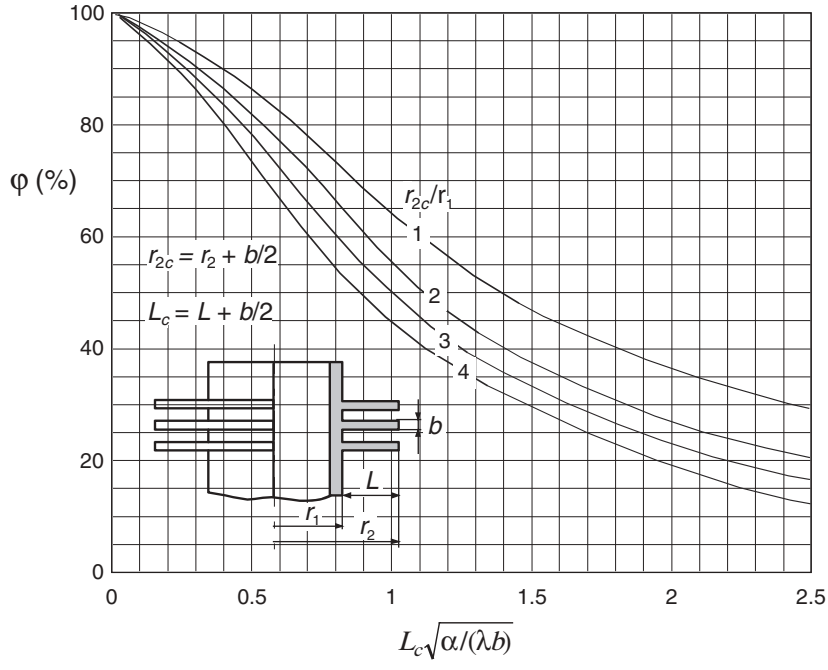

Fig. 5. Fin efficiency for annular fins.

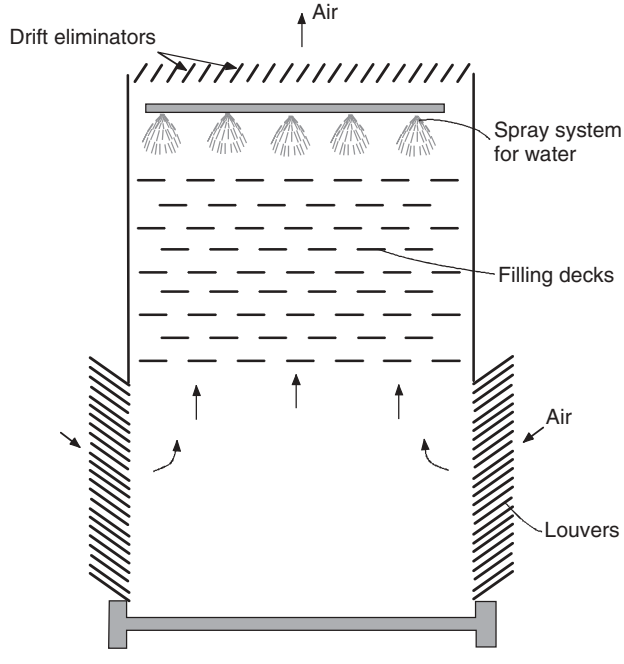

Fig. 6. Cooling tower where the air movement is by natural convection.

Fig. 7. Compact heat exchanger. (Radiator for a private car.)

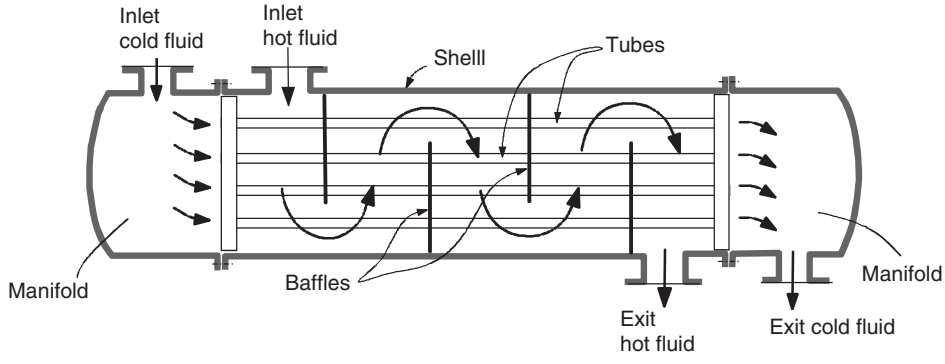

Fig. 8. Principle sketch of a shell-and-tube heat exchanger. One shell pass and one tube pass.

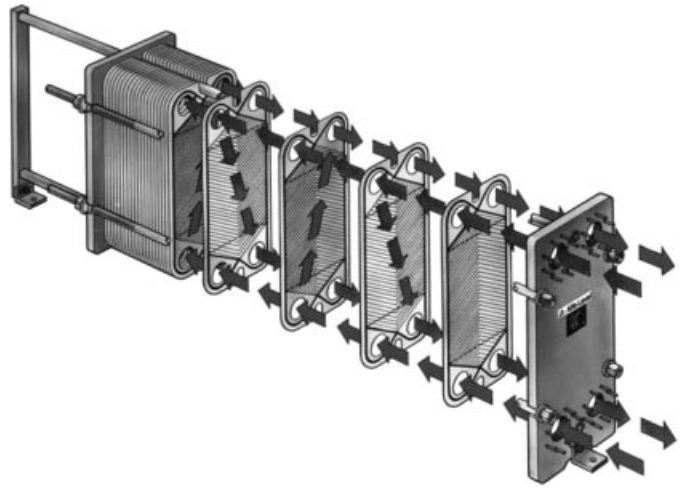

Fig. 9. Plate heat exchanger. (From Alfa Laval AB.)

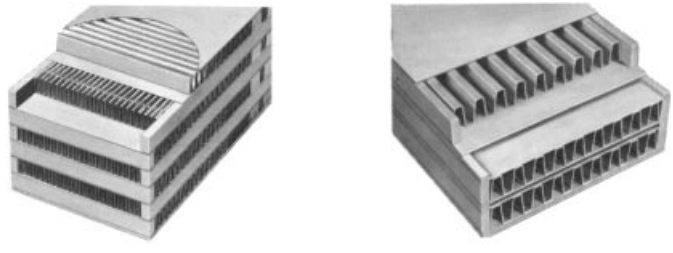

Fig. 10. Finned plate heat exchangers. (From Harrison Radiator Division, General Motors.)

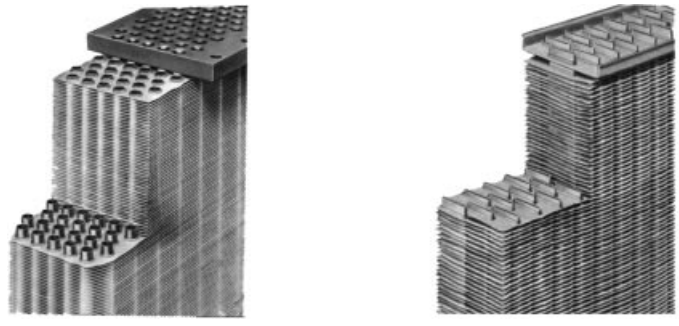

Fig. 11. Finned tubular heat exchangers. (From Harrison Radiator Division, General Motors.)

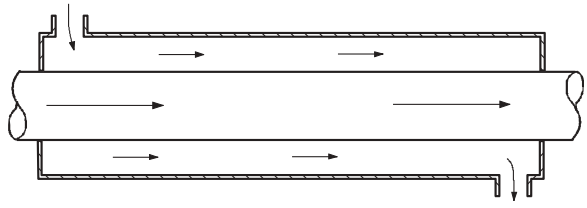

Fig. 12. Cocurrent or parallel flow heat exchanger.

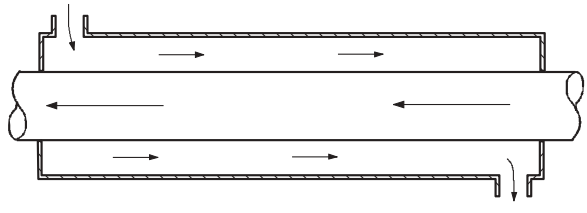

Fig. 13. Counterflow arrangement.

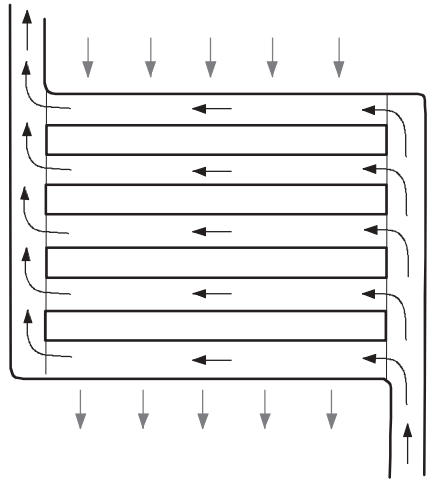

Fig. 14. Simple cross-flow arrangement.

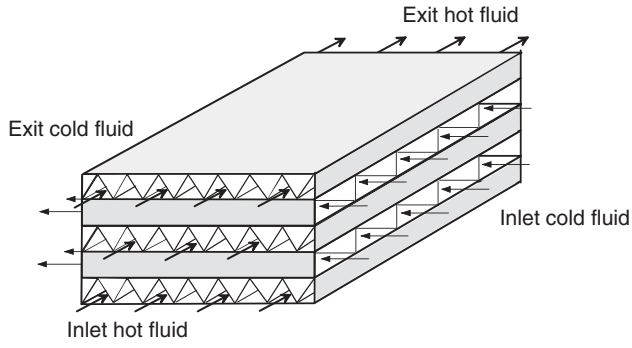

Fig. 15. Cross-flow heat exchangers. Both media are unmixed.

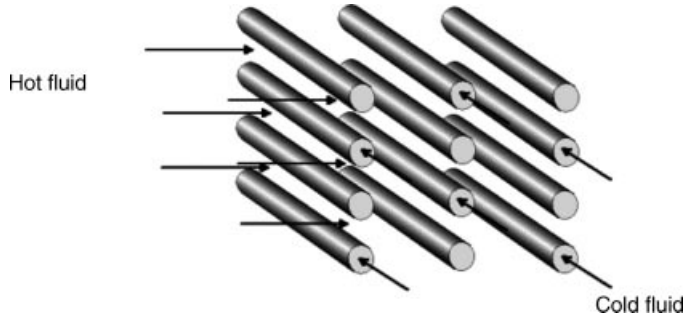

Fig. 16. One fluid unmixed, one mixed.

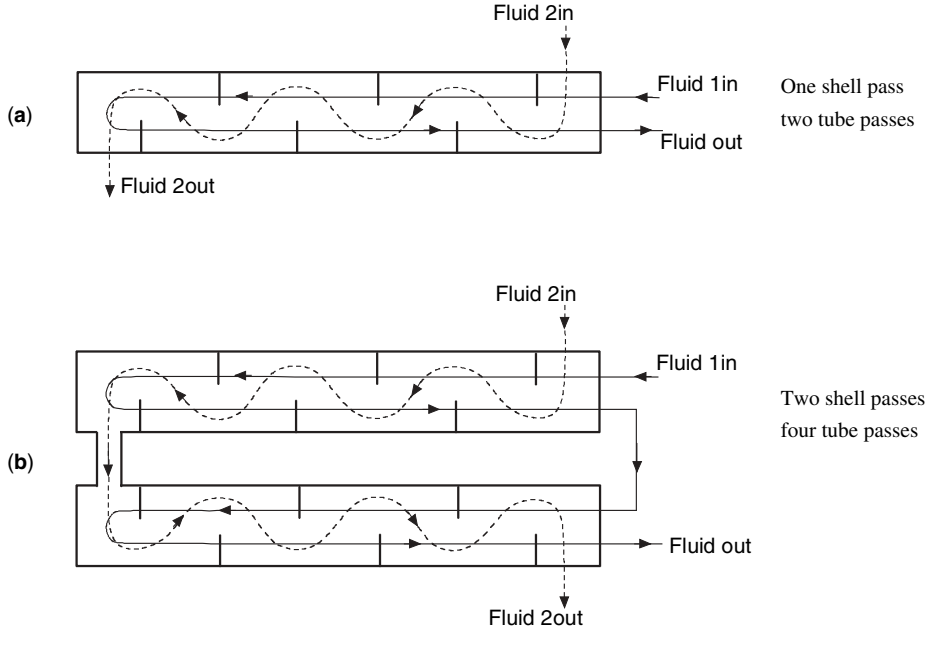

Fig. 17. Common multipass arrangements.

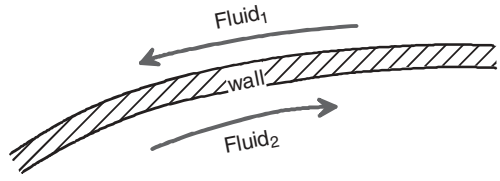

Fig. 18. Principle sketch of the heat transfer process.

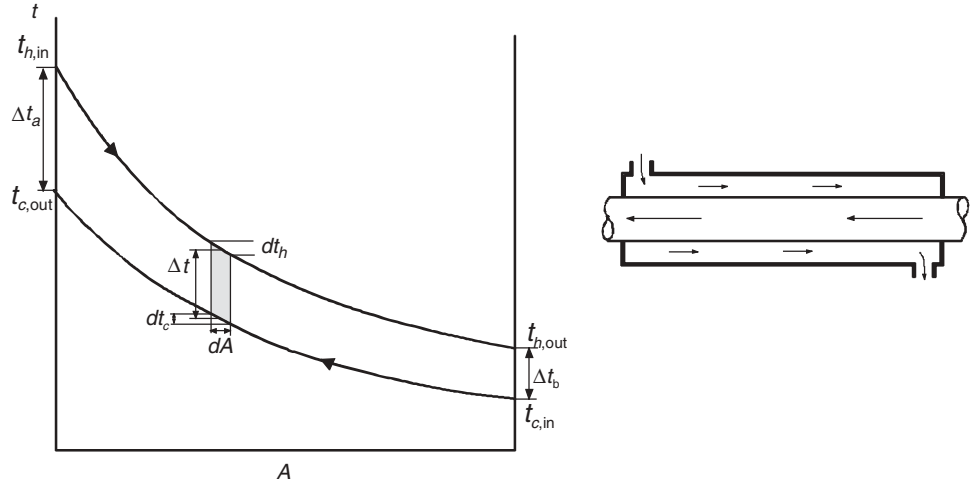

Fig. 19. Principle sketch of temperature distributions in a counterflow heat exchanger.

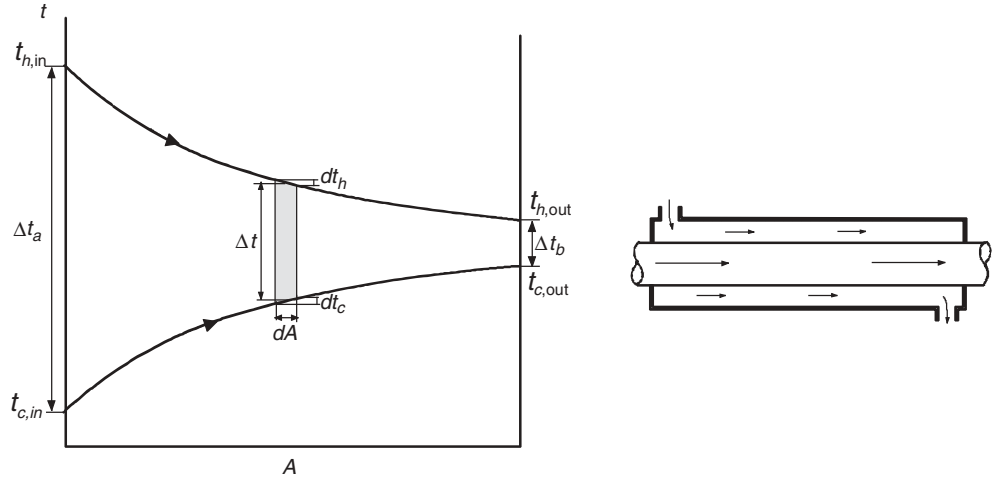

Fig. 20. Principle sketch a parallel flow heat exchanger.

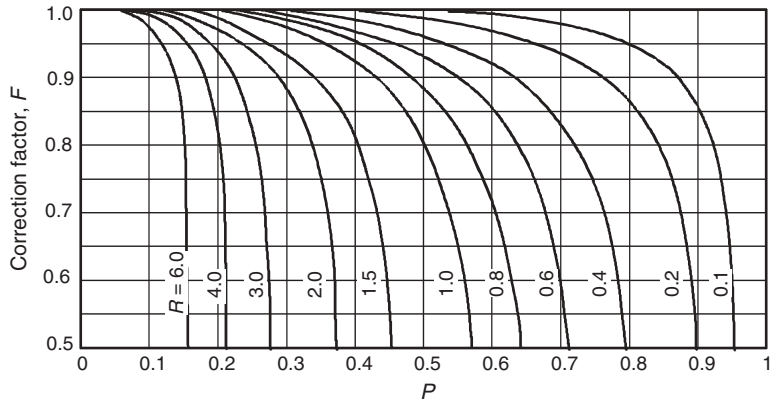

Fig. 21. Correction factor F for a shell-and-tube heat exchanger with one shell pass and two tube passes. From (2).

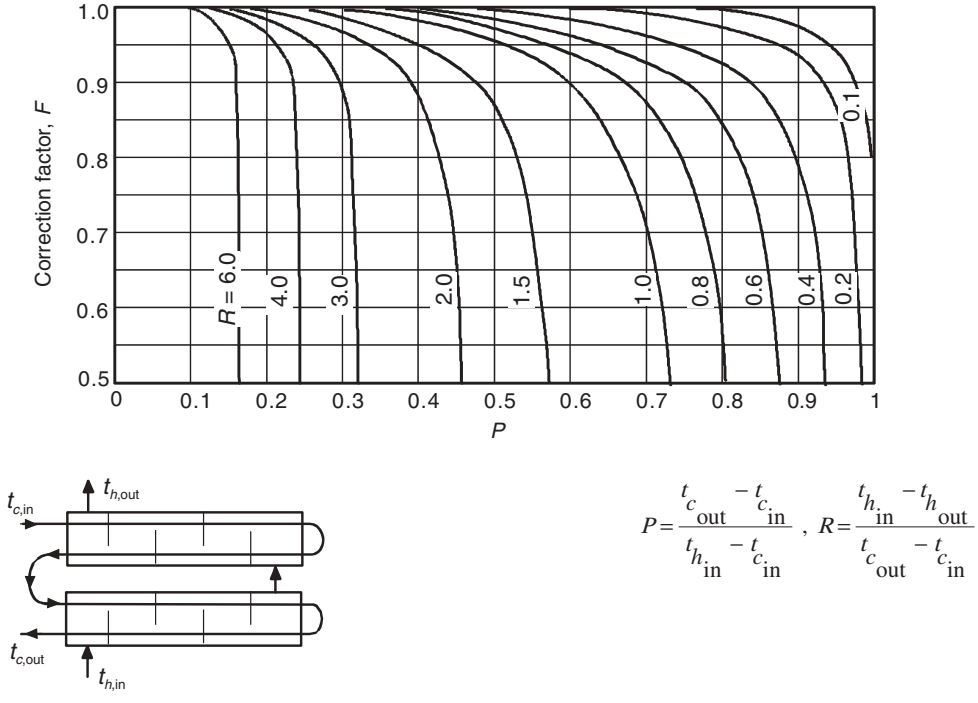

Fig. 22. Correction factor F for a shell-and-tube heat exchanger with two shell passes and four tube passes. From (2).

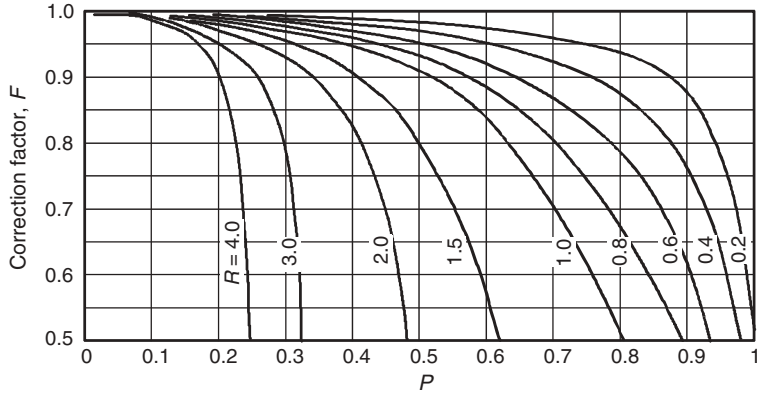

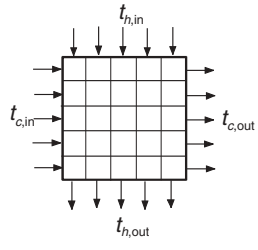

$$P = \frac{t_{c\,\text{out}} - t_{c\,\text{in}}}{t_{h\,\text{in}} - t_{c\,\text{in}}}, \quad R = \frac{t_{h\,\text{in}} - t_{h\,\text{out}}}{t_{c\,\text{out}} - t_{c\,\text{in}}}$$

Fig. 23. Correction factor F for a cross-flow heat exchanger with both fluids unmixed. From (2).

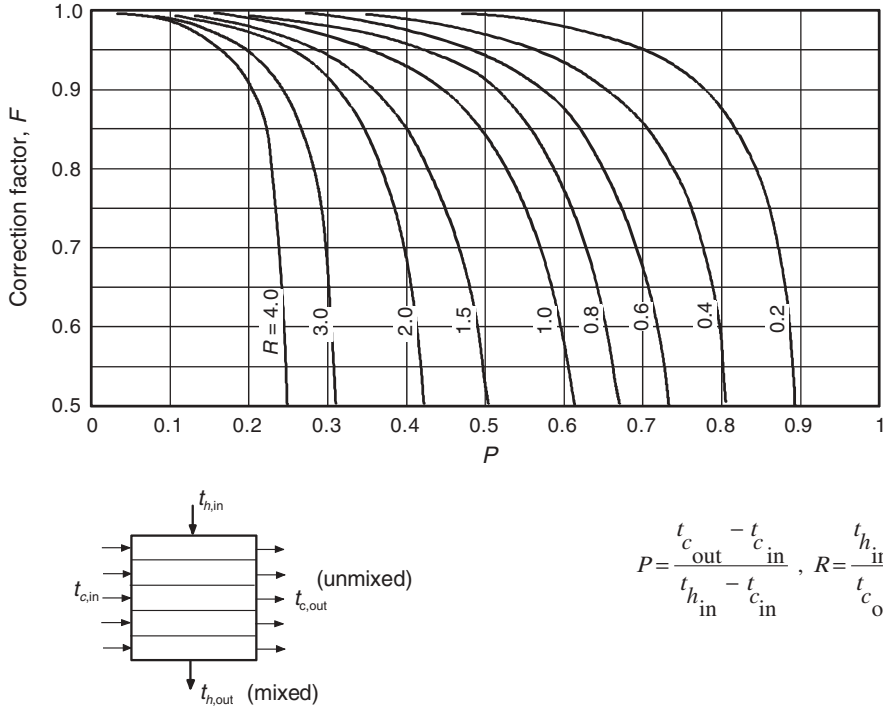

$$P = \frac{t_{c_{out}} - t_{c_{in}}}{t_{h_{in}} - t_{c_{in}}}, \quad R = \frac{t_{h_{in}} - t_{h_{out}}}{t_{c_{out}} - t_{c_{in}}}$$

Fig. 24. Correction factor F for across flow heat exchanger with one fluid unmixed. From (2).

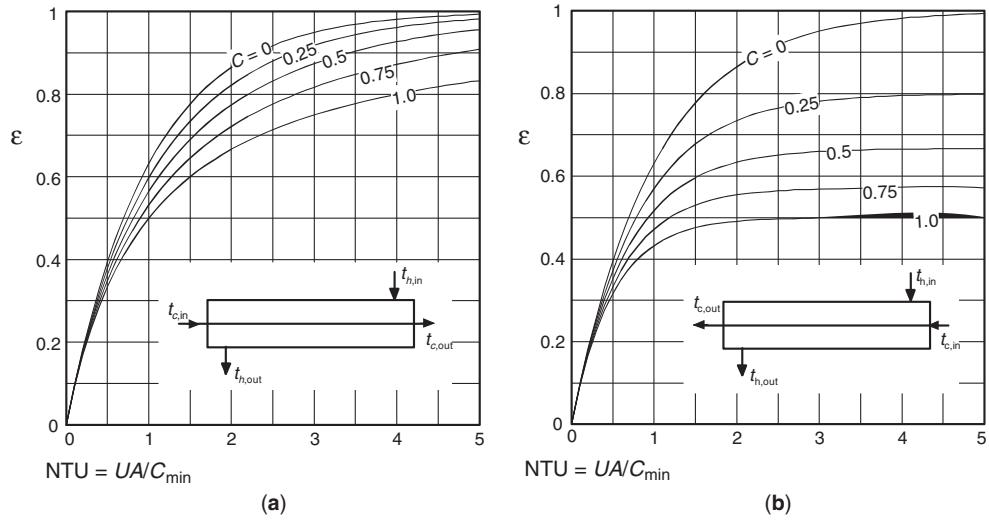

Fig. 25. (**a**) ε-NTU for a counter flow heat exchanger. From (2) (**b**) ε-NTU for a parallel flow heat exchanger. From (2).

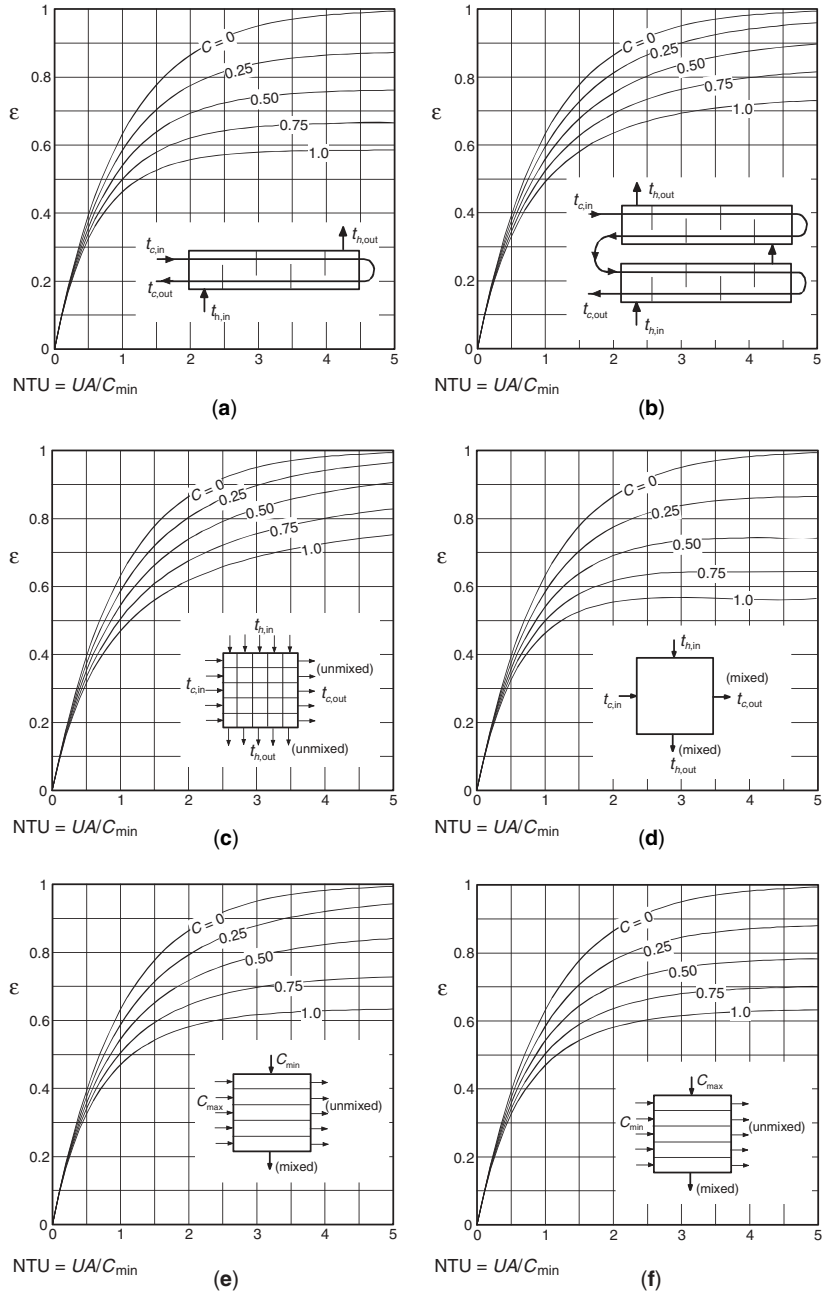

Fig. 26. (**a**) ε-NTU for shell-and-tube heat exchangers with one shell pass and two tube passes. From (2) (**b**) ε-NTU for shell-and-tube heat exchangers with two shell passes and four tube passes. From (2) (**c**) ε-NTU for cross-flow heat exchangers with both fluids unmixed. From (2) (**d**) ε-NTU for cross flow heat exchangers with both fluids mixed. From (2) (**e**) ε-NTU for cross-flow heat exchangers, where the fluid with $C_{\min}$ is mixed while the other is unmixed. From (2) (**f**) ε-NTU for cross-flow heat exchangers, where the fluid with $C_{\max}$ is mixed, while the other is unmixed. From (2).

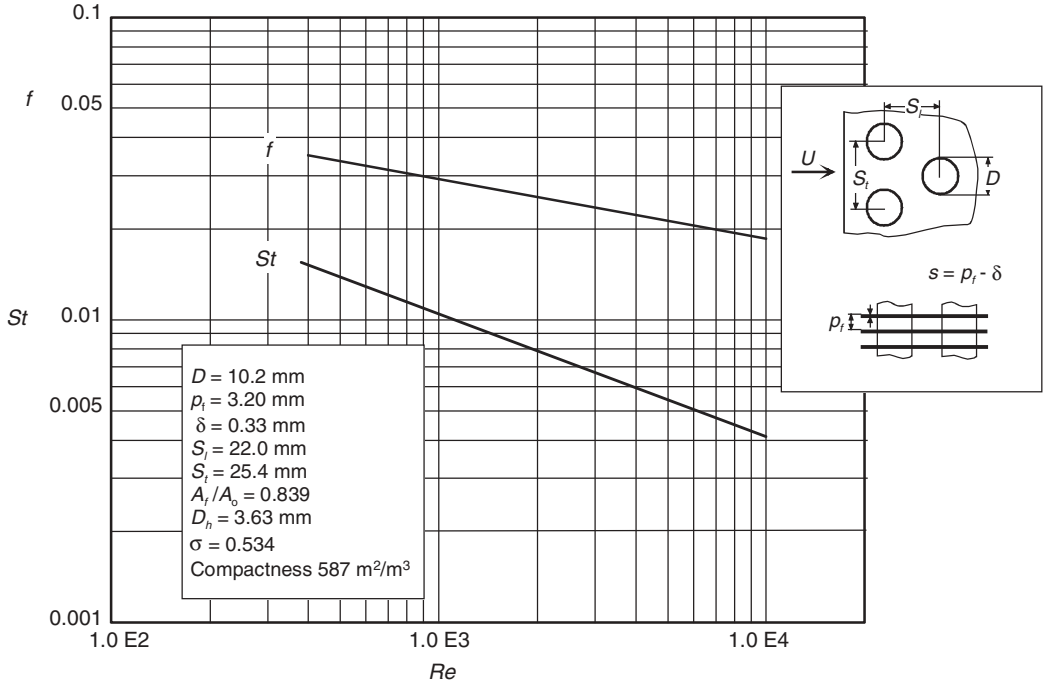

Fig. 27. Stanton number, *St*, and friction factor, *f*, for a finned tubular heat exchanger From (13).

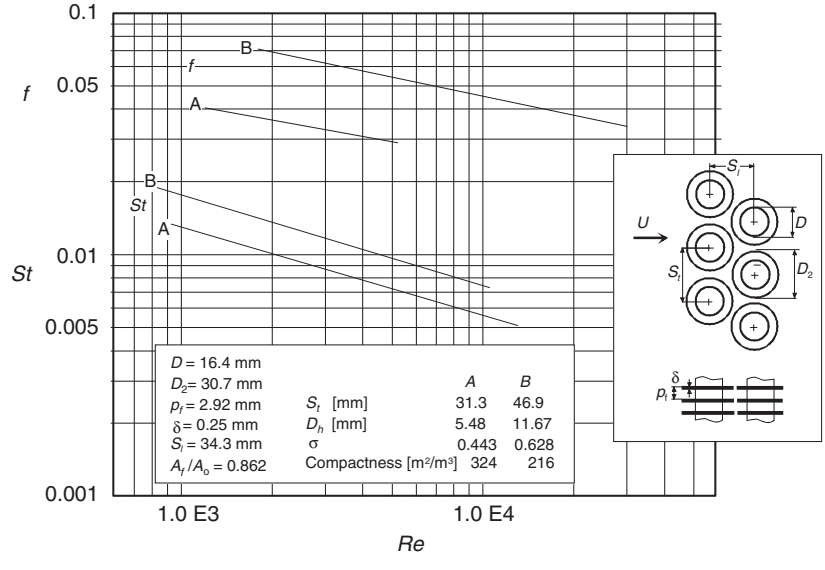

Fig. 28. Stanton number, *St*, and friction factor, *f*, for a tubular heat exchanger with plane fins. From (13).

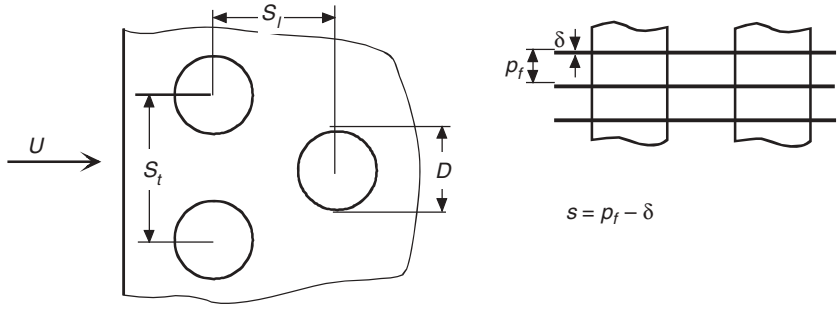

Fig. 29. Notations for tubular heat exchangers with plane fins.

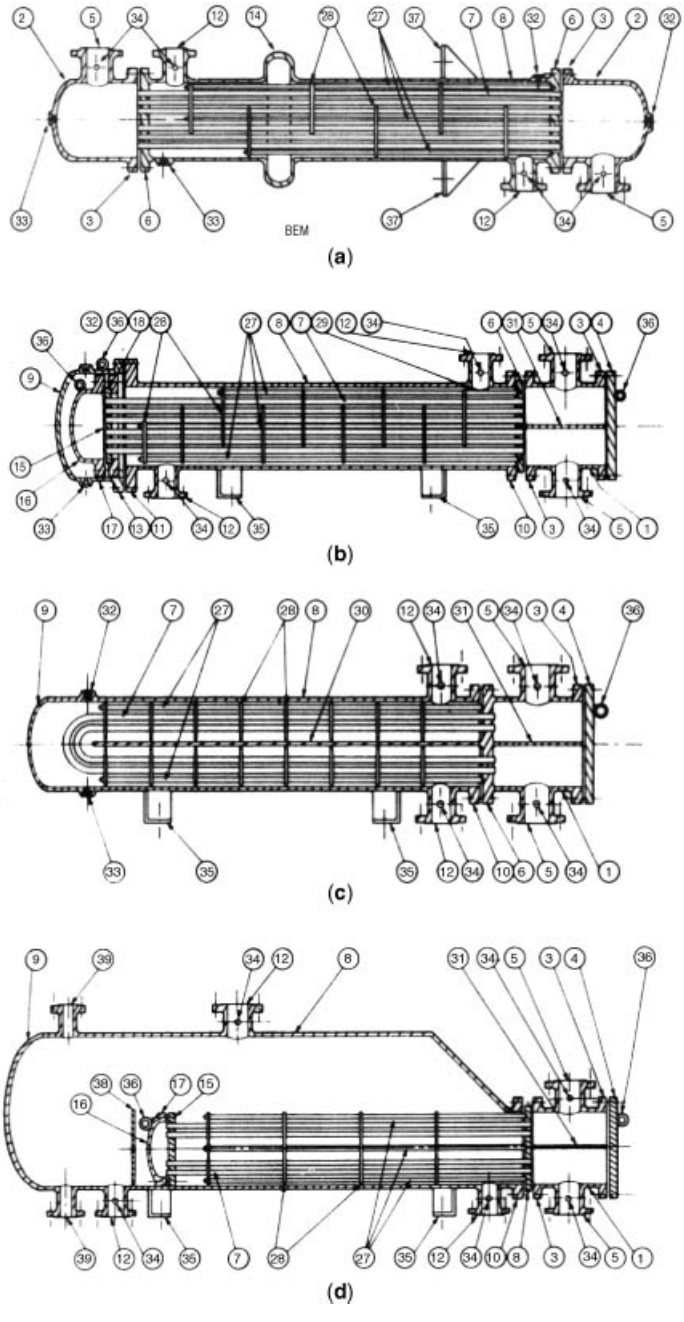

Fig. 30. (**a**) Shell-and- tube heat exchangers, one shell pass and one tube pass. (**b**) Shell-and-tube heat exchanger, one shell pass and two tube passes, mixing between the tube passes. (From TEMA-Tubular Exchanger Manufacturer Association.) (**c**) Shell-and-tube heat exchangers. one shell pass and two tube passes, without mixing between the tube passes. (**d**) Shell-and-tube heat exchanger, Kettle-reboiler.

1. Stationary head-channel
2. Stationary head-bonnet

3. Stationary head-flang-channel or bonnet
4. Channel cover
5. Stationary head nozzle
6. Stationary tube-sheet
7. Tubes
8. Shell
9. Shell cover
10. Shell flange-stationary head end
11. Shell flange-rear head end
12. Shell nozzle
13. Shell cover flange
14. Expansion joint
15. Floating tube-sheet
16. Floating head cover
17. Floating head flange
18. Floating head backing device
19. Split shear ring
20. Slip-on backing flange
21. Floating head cover-external
22. Floating tube-sheet skirt
23. Packing box
24. Packing
25. Packing gland
26. Lantern ring
27. Tierods and spacers
28. Transverse baffles or support plates
29. Impingement plate
30. Longitudinal baffle
31. Pass partition
32. Vent connection
33. Drain connection
34. Instrument connection
35. Support saddle
36. Lifting lug
37. Support bracket
38. Weir
39. Liquid level connection

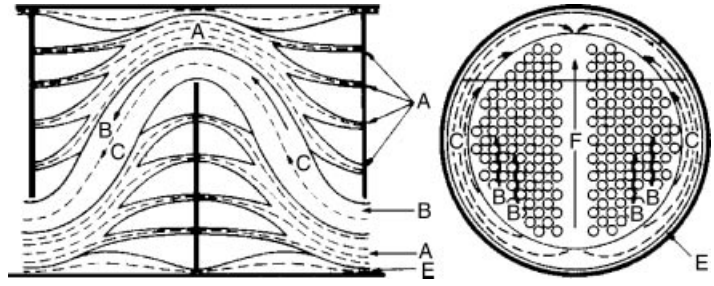

Fig. 31. Tinker's sketch of the flow field on the shell side in a shell-and-tube heat exchanger.

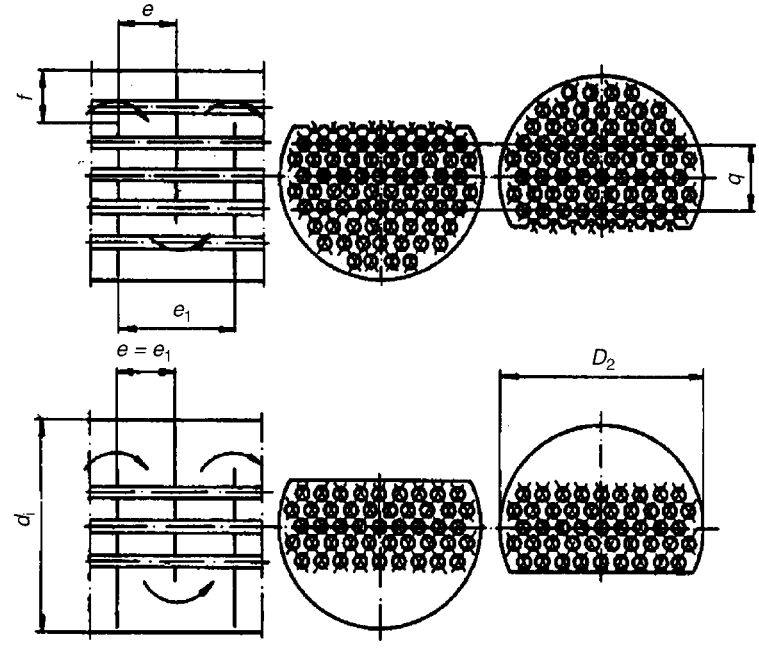

Fig. 32. Baffle designs.

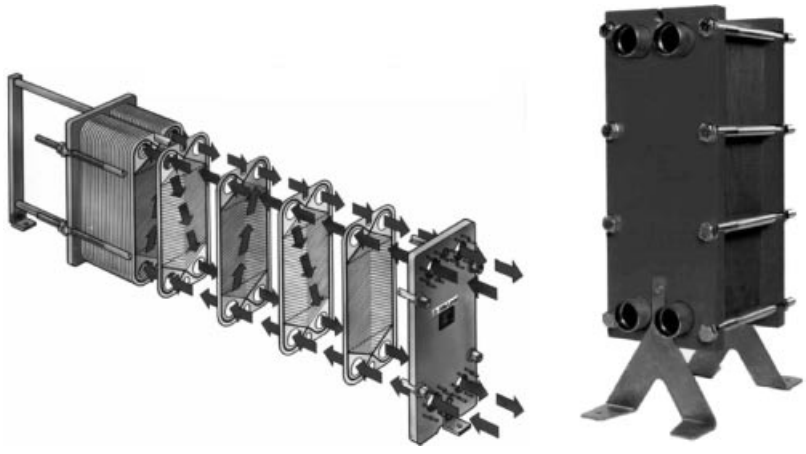

Fig. 33. Plate heat exchanger.

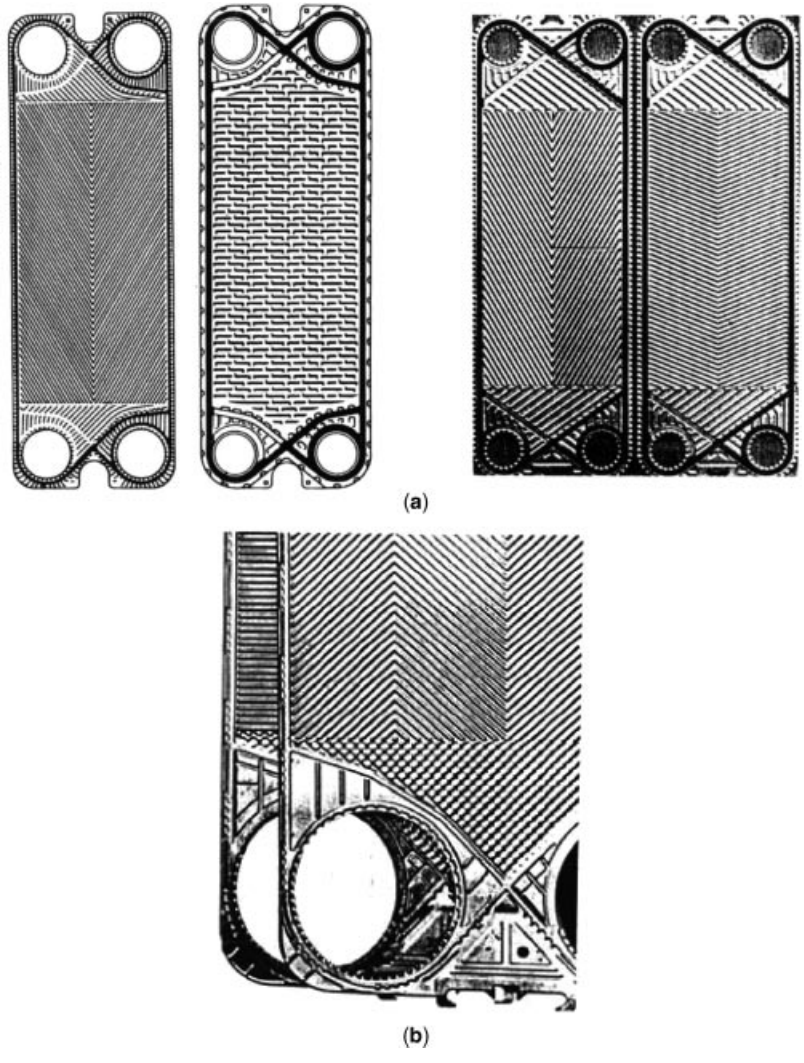

Fig. 34. (**a**) Plate pattern; (**b**) Plate pattern.

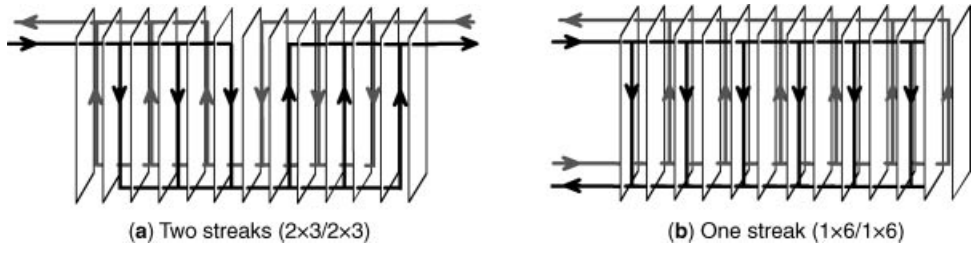

Fig. 35. Flow streaks.

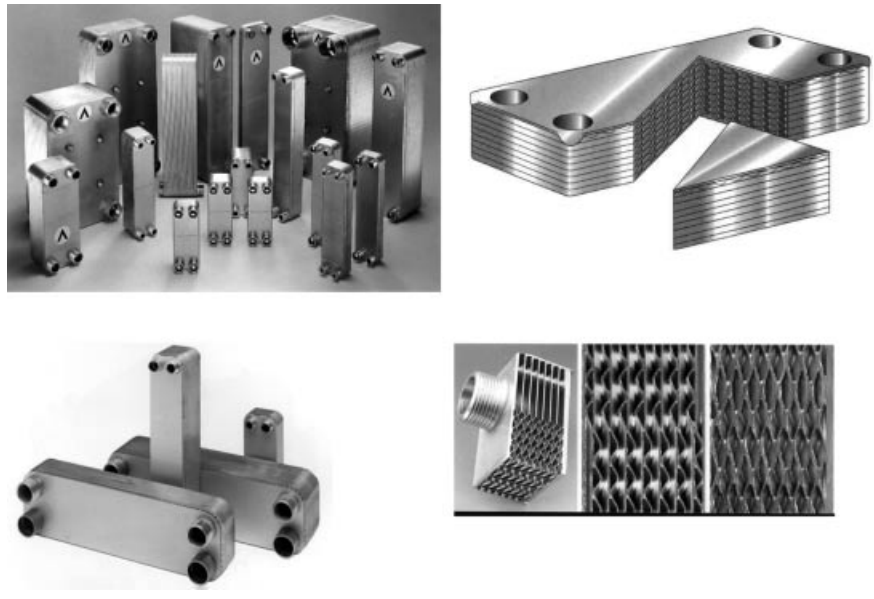

Fig. 36. Brazed PHEs.

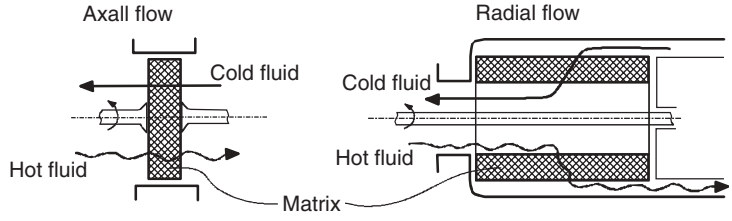

Fig. 37. Rotating regenerative heat exchanger.

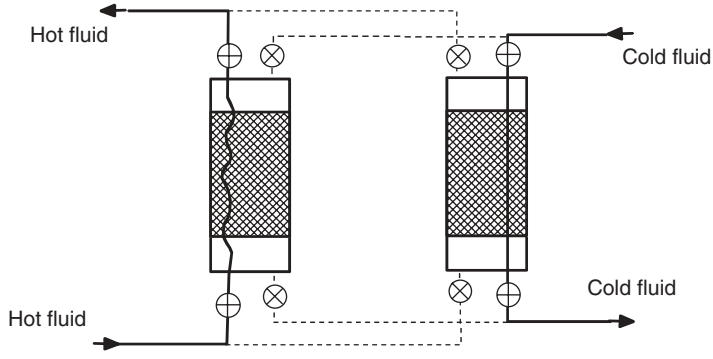

Fig. 38. Static regenerative heat exchanger.

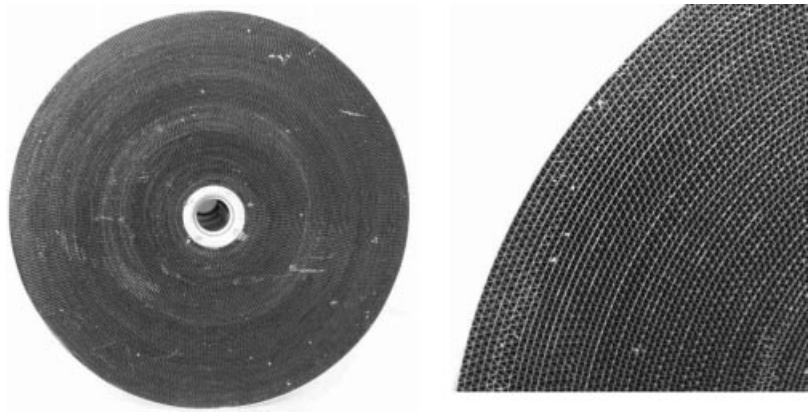

Fig. 39. The wheel or rotor of a rotating regenerative heat exchanger.

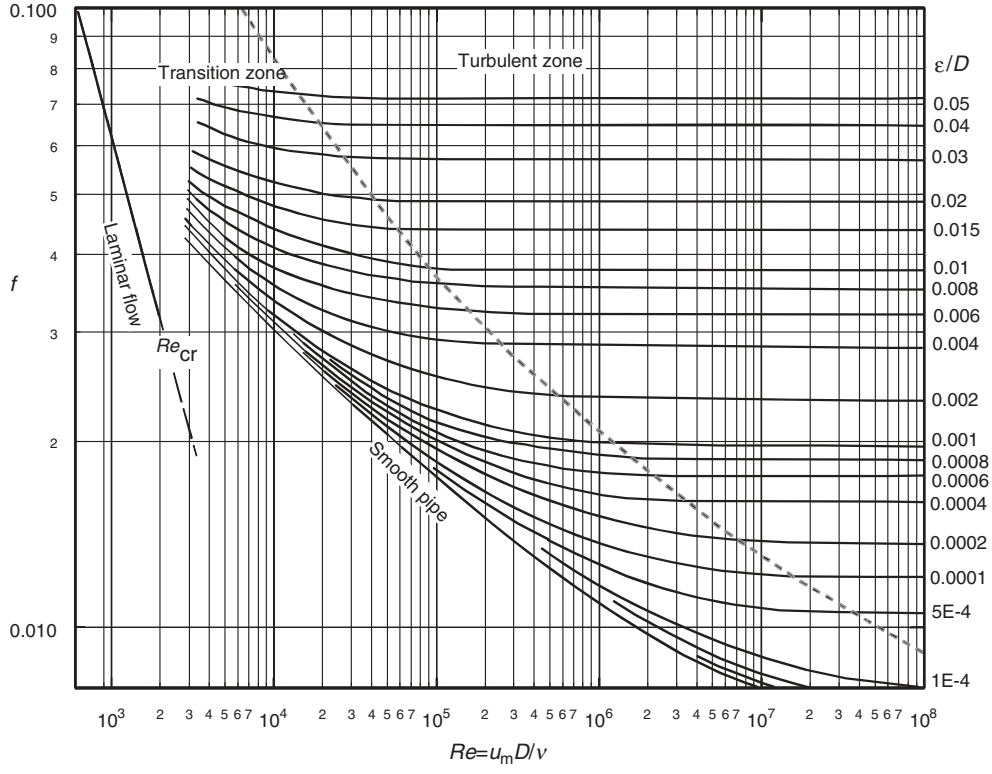

Fig. 40. The friction factor f for pipe flow according to Moody (29,30).

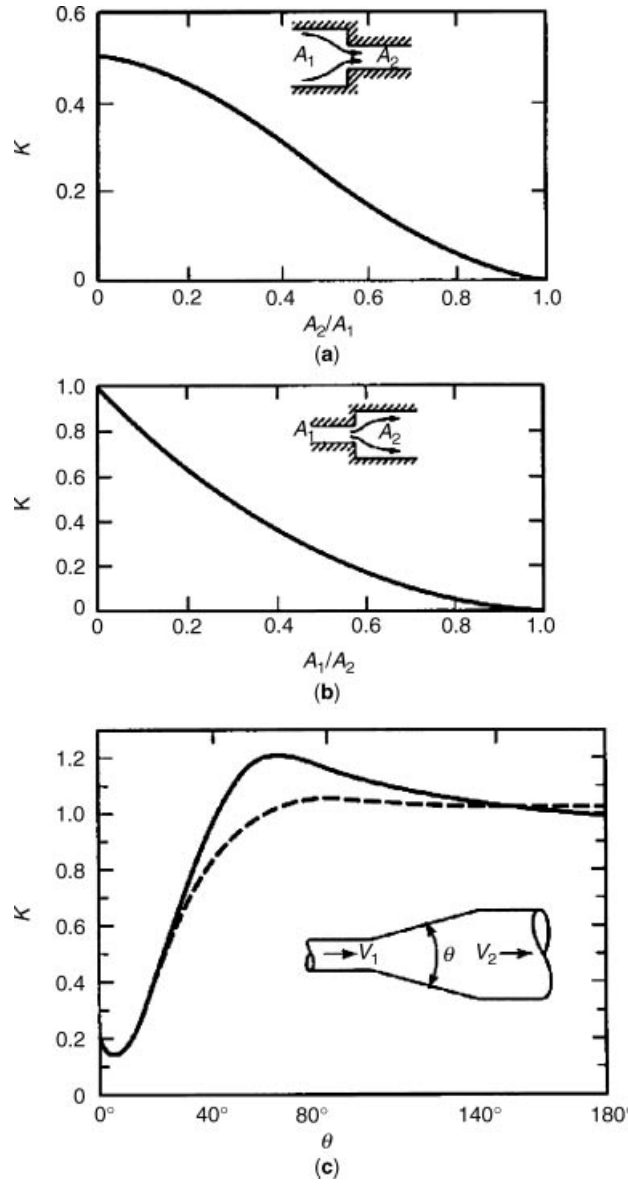

Fig. 41. Pressure loss coefficient, K (**a**) for sudden contraction, $(\Delta p) = K(\frac{1}{2}\rho V_2^2)$; (**b**) for sudden expansion, $(\Delta p) = K(\frac{1}{2}\rho V_1^2)$; (**c**) versus θ in a gradually expanding section $(\Delta p) = K(\frac{1}{2}\rho(V_1^2 - V_2^2))$, where (--------) $D_2/D_1 = 1.5$; (- - - - -), $D_2/D_1 = 3$ (29).

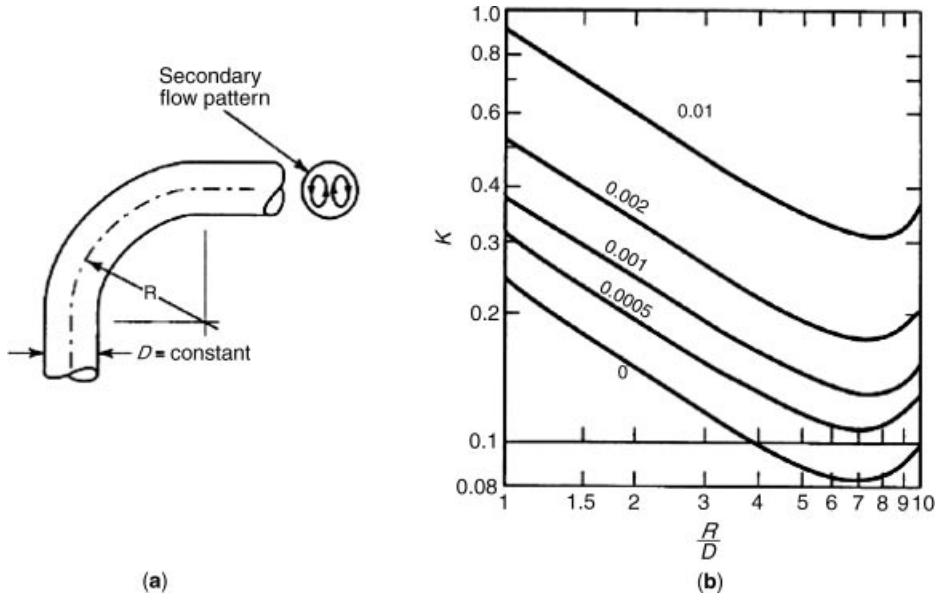

Fig. 42. (**a**) Configuration for flow turning. The frictional resistance resulting from the bend length must be added; (**b**) pressure–loss coefficient, K, for 90° flow turning where the numbers on the lines refer to η/D values. (30).